GEOLOGICAL SURVEY OF CANADA
BULLETIN 499

COLOUR ALTERATION, THERMAL MATURITY, AND BURIAL DIAGENESIS IN FOSSIL FORAMINIFERS

D.H. McNeil, D.R. Issler, and L.R. Snowdon

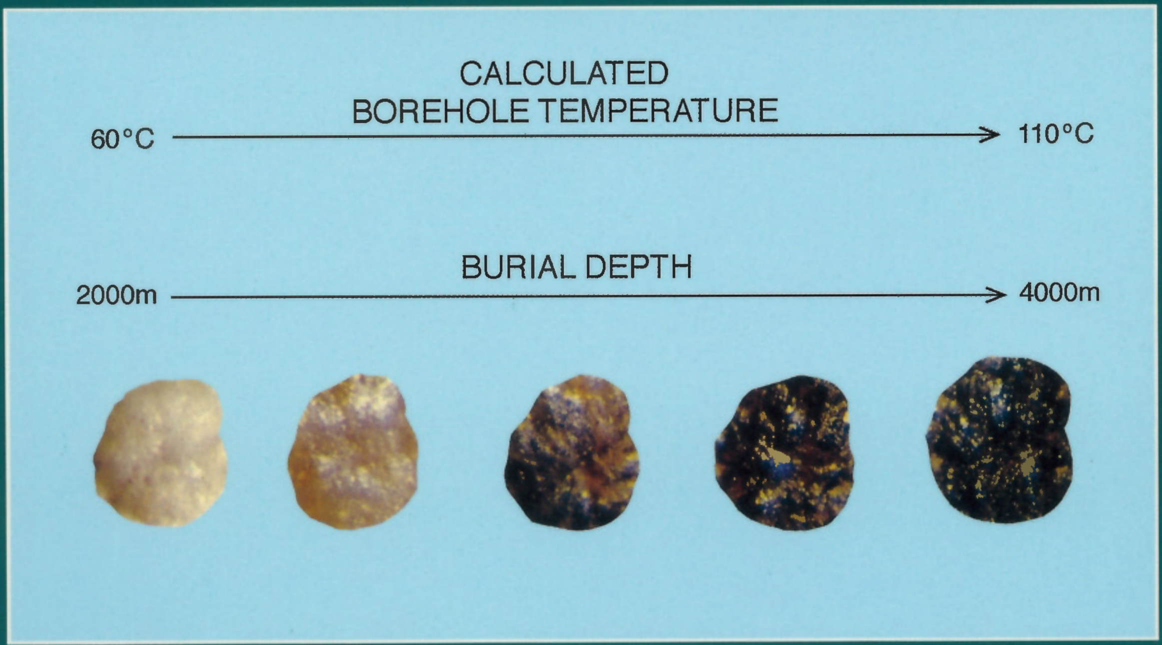

1996

Natural Resources Canada
Ressources naturelles Canada

Canada

GEOLOGICAL SURVEY OF CANADA
BULLETIN 499

COLOUR ALTERATION, THERMAL MATURITY, AND BURIAL DIAGENESIS IN FOSSIL FORAMINIFERS

D.H. McNeil, D.R. Issler, and L.R. Snowdon

1996

Catalogue No. M42-499E
ISBN 0-660-16451-5

Available in Canada from

Geological Survey of Canada offices:

601 Booth Street
Ottawa, Ontario K1A 0E8

3303 - 33rd Street N.W.
Calgary, Alberta T2L 2A7

100 West Pender Street
Vancouver, B.C. V6B 1R8

or from

Canada Communication Group–Publishing
Ottawa, Canada K1A 0S9

and through authorized bookstore agents
and other bookstores

A deposit copy of this publication is also available for reference
in public libraries across Canada

Price subject to change without notice

Cover Illustration
Typical colour sequence recognized in fossil foraminifers from the Beaufort–Mackenzie Basin, arctic Canada. Specimens GSC 112229–112233 from the Amauligak J-44 well, see Figure 9, page 12.

Critical readers

D.W. Morrow
J. Utting

Author's address

Geological Survey of Canada (Calgary)
3303 - 33 Street N.W.
Calgary, Alberta
T2L 2A7

Manuscript submitted: 95.11.03
Approved for publication: 96.05.17

PREFACE

Thermal maturity studies are an integral part of sedimentary basin analysis and hydrocarbon exploration. Conventional methods for measuring thermal maturity, such as vitrinite reflectance, have long been applied by petroleum explorationists and organic petrologists. In this report, new methods are introduced for assessing thermal maturity based on colour and mineralogical changes in foraminifers (microfossils that are biostratigraphically important elements in marine sedimentary sequences). Microfossils already play a key role in basin analysis, since they have unique time and space significance. The interpretation of foraminiferal burial diagenesis adds to the overall usefulness of microfossils and enhances their value as a predictive tool in hydrocarbon exploration. The methods and techniques presented here were based on studies in Canada's frontier Beaufort–Mackenzie Basin. The results, however, are applicable to marine sedimentary basins in other regions of Canada and around the world. These results confirm NRCan's commitment to providing topical research on the petroleum basins of Canada.

M.D. Everell
Assistant Deputy Minister
Earth Sciences Sector

PRÉFACE

Les études sur la maturité thermique font partie intégrante des travaux d'analyse des bassins sédimentaires et d'exploration des hydrocarbures. Depuis longtemps, les géologues se consacrant à l'exploration du pétrole et les pétrologues spécialisés dans les roches d'origine organique ont fait appel aux méthodes classiques pour mesurer la maturité thermique, comme celle dont le fondement est le pouvoir réflecteur de la vitrinite. Le présent bulletin décrit de nouvelles méthodes d'évaluation de la maturité thermique, notamment les changements de couleur et de minéralogie observés dans les foraminifères (microfossiles ayant une importance biostratigraphique dans les séquences sédimentaires marines). Les microfossiles jouent déjà un rôle clé dans l'analyse des bassins, en raison des renseignements spatio-temporels uniques qu'ils recèlent. L'interprétation de la diagenèse par enfouissement des foraminifères accroït l'utilité globale des microfossiles et leur donne plus d'importance comme outil de prévision en exploration des hydrocarbures. Les méthodes et les techniques présentées ici sont illustrées dans le cadre des études faites dans le bassin de Beaufort-Mackenzie, l'une des régions pionnières du Canada. Cependant, les résultats peuvent s'appliquer aux bassins sédimentaires marins d'autres régions du pays et d'ailleurs dans le monde. Ces résultats confirment l'engagement de RNCan à mener des recherches spécialisés sur les bassins pétrolifères du Canada.

M.D. Everell
Sous-ministre adjoint
Commission geologique du Canada

CONTENTS

1 Abstract/Résumé
2 Summary
3 Sommaire
5 Introduction
5 Acknowledgments
5 Organic matter in the foraminiferal test
6 Samples
7 Observations and hypotheses
9 Quantification of colour alteration
12 Experimental versus geothermal colour alteration
16 Burial diagenesis and mineralization in fossil foraminifers
20 Origin of mineralogical changes
21 FCI, zones of burial diagenesis, and thermal maturity
22 FCI trends in six exploration wells
22 General trends
22 Offshore wells
25 Onshore wells
27 Concluding remarks
28 References
30 Appendix 1: Foraminiferal colouration index (FCI) data for seven exploration wells in the Beaufort–Mackenzie Basin
33 Appendix 2: List of illustrated type specimens and locality information

Figures

6 1. Planktonic foraminifers agglutinated to the arenaceous test of *Rhabdammina*
6 2. Detail of agglutinated grains in the wall of Holocene *Rhabdammina*
7 3. Map of study area, well and outcrop locations
7 4. Stratigraphic units of the Beaufort–Mackenzie Basin and sample distribution
8 5. Typical colour sequence recognized in fossil foraminifers from the Beaufort–Mackenzie Basin, arctic Canada
8 6. Micrographs showing progressive alteration of the test wall of agglutinated foraminifers by secondary development of quartz (silicification) with increasing burial diagenesis
10 7. Micrographs showing alteration of the test wall of calcareous foraminifers through recrystallization and chloritization with increasing burial diagenesis
11 8. Foraminiferal Colouration Index (FCI) calibrated against colour chips from the Munsell Soil Colour Chart
12 9. Thermal maturity indices (FCI, VRo%, Tmax) and total organic carbon measured from cuttings samples in the Amauligak J-44 well, central Beaufort Sea
13 10. Thermal maturity indices (FCI, VRo%, Tmax) and total organic carbon measured from core samples from the Issungnak 2O-61 well, central Beaufort Sea
14 11. Thermal maturity indices (FCI, VRo%, Tmax) and total organic carbon measured from core samples from the Roland Bay L-41 well, northern Yukon Territory
15 12. Examples of colour in microfossils
15 13. Colour alteration effects in microfossils after heating by pyrolysis
16 14. Examples of fossil colouration before and after heating by pyrolysis
17 15. Comparison of colouration effects before and after pyrolysis heating in the presence of air, in a helium atmosphere, and for oil-stained specimens in helium
18 16. Burial diagenesis in foraminifers
19 17. Generalized burial diagenetic trends observed in the organic matter and mineralogy of agglutinated and calcareous foraminifers
20 18. *Lenticulina* coated with black bituminous residue, interior filled by whitish chloritic clay
20 19. EDX identification of secondary clay mineralization in fossil foraminifers at relatively high levels of burial diagenesis

21 20. Pyramidal quartz overgrowths around a primary grain in the wall of an agglutinated foraminifer (*Reticulophragmium*, Amauligak J-44, 3998 m)
23 21. Distribution of Foraminiferal Colouration Index (FCI) in six Beaufort–Mackenzie exploration wells
24 22. Temperature versus depth for four offshore Beaufort–Mackenzie exploration wells
25 23. Present temperature versus FCI for four offshore Beaufort–Mackenzie exploration wells
26 24. Comparison of the distribution of FCI and porosity trends in the Reindeer D-27 well, Mackenzie Delta

Table

11 1. Foraminiferal Colouration Index (FCI) compared to standard colour sequence from Munsell Soil Colour Chart

COLOUR ALTERATION, THERMAL MATURITY, AND BURIAL DIAGENESIS IN FOSSIL FORAMINIFERS

Abstract

Foraminifers are potentially sensitive indicators of thermal maturity. Changes in colour of the organic cement in the agglutinated test, and mineralogical changes in agglutinated and calcareous benthic foraminifers, provide evidence of thermal alteration.

Empirical data from fossil specimens, and pyrolysis experiments, both indicate that darker colouration is related to thermal alteration. Colour changes can be measured accurately and quantitatively by comparison with the standard Munsell Colour Chart. An index consisting of ten categories has been established and is named the Foraminiferal Colouration Index (FCI). Examination of FCI in exploration wells in the Beaufort–Mackenzie Basin of arctic Canada indicate that FCI is most sensitive at levels of maturation equivalent to the early stages of petroleum generation. It also indicates that FCI may be retarded, or even reversed, by the influence of pore fluids in overpressured zones. Furthermore, FCI appears to be sensitive to heating rate, with the most rapidly deposited sediments showing the least increase in FCI with temperature.

Mineralogical changes within the tests of both agglutinated and calcareous benthic foraminifers can be caused by diagenetic alteration. Based on data from exploration wells in the Beaufort–Mackenzie Basin, four zones of burial diagenesis (A–D) have been recognized. Zone A is characteristic of burial depths less that 2400 m (less than 75°C), wherein fossil foraminifers show little or no alteration. Zone B, at burial depths of 2400 to 3500 m (75 to 110°C), is characterized primarily by quartz mineralization (silicification). Zone C, at burial depths of 3500 to 5000 m (110–140°C), is characterized by further silicification and precipitation of kaolin and smectite in foraminiferal tests. Zone D, at estimated burial depths of 6 to 8 km (150–250°C), is recognized by intense silicification, recrystallized calcite, and precipitation of illite and chlorite. Calcareous specimens in Zone D are particularly unstable and may be replaced entirely by chloritic clay (chloritized).

Résumé

Les foraminifères pourraient étre de bons indicateurs de la maturité thermique. Cela parce que les changements de couleur du ciment organique dans le test agglutinant et les changements minéralogiques observés dans les foraminifère benthiques à test tant agglutinant que calcaire témoignent de l'altération thermique.

Des données empiriques sur des spécimens fossiles et des expériences par pyrolyse indiquent que la coloration foncée est liée à une altération thermique. Les changements de couleur peuvent se mesurer avec précision et de façon quantitative en utilisant le système de classification des couleurs de Munsell. Un indice comportant dix catégories a été établi; il s'appelle l'«indice de coloration des foraminifères» (ICF). Son examen dans les puits d'exploration forés dans le bassin de Beaufort-Mackenzie (Arctique canadien) révèle que sa sensibilité est plus élevée aux niveaux de maturation correspondant aux premiers stades de genèse du pétrole. Il indique en outre que l'ICF peut étre décalé, ou méme inversé, par les fluides interstitiels présents dans les zones en surpression. De plus, l'ICF semble étre sensible au taux d'augmentation de la température, les sédiments déposés les plus rapidement montrant la plus faible augmentation de l'ICF en fonction de la température.

Les changements minéralogiques au niveau des tests tant agglutinants que calcaires des foraminifères benthiques peuvent avoir été causés par une altération diagénétique. Les données des puits forés dans le bassin de Beaufort-Mackenzie ont permis de dégager quatre zones de diagenèse par enfouissement (A-D). La zone A représente des profondeurs d'enfouissement de moins de 2 400 m (moins de 75 °C) et les foraminifères fossiles y sont peu ou pas altérés. La zone B, correspondant à des profondeurs d'enfouissement de 2 400 à 3 500 m (entre 75 et 110 °C) se distingue surtout par la présence de quartz secondaire (silicification). La zone C (profondeurs de 3 500 à 5 000 m et températures de 110 à 140 °C) se caractérise par une silicification accrue ainsi que la précipitation de kaolinite et de smectite dans les tests des foraminifères. Dans la zone D, dont les profondeurs d'enfouissement vont de 6 à 8 km (150-250 °C), la silicification est intense et il y a recristallisation de calcite ainsi que précipitation d'illite et de chlorite. Les spécimens calcaires présents dans la zone D sont particulièrement instables et peuvent étre entièrement chloritisés.

Summary

Two new schemes for assessing thermal maturity are introduced in this paper. The first scheme is referred to as the Foraminiferal Colouration Index (FCI) and is based on thermally induced colour changes in the organic cement of agglutinated foraminifers. The second scheme is a burial diagenetic zonation based on generalized mineralogical changes in foraminifers resulting from geothermal and hydrothermal effects. These include precipitation of secondary quartz (overgrowths), precipitation of clay minerals such as smectite, kaolinite, illite, and chlorite, and recrystallization and replacement of calcite.

Comparison of FCI data with vitrinite reflectance and Rock-Eval data indicates that foraminiferal colour is most sensitive to change in the early stages of petroleum generation. Silicification of the foraminiferal test also begins to occur in this stage, so that foraminiferal preservation is an easily recognizable indicator of the onset of hydrocarbon generation.

Foraminifers are common in Mesozoic–Cenozoic, marine, and terrigenous, sedimentary rocks of the Beaufort–Mackenzie Basin. The fossil record clearly indicates that foraminifers undergo progressive changes in colouration and mineralization as thermal maturity increases. Colouration changes, which range from white through shades of greyish amber-brown to black, result from the thermal maturation of the organic cement (glycosaminoglycan) that surrounds every grain within the agglutinated test and may coat the inner and outer surfaces of the entire test. The preservation of organic cement in the fossil record is revealed through standard SEM observation. Etching of the foraminiferal test with hydrofluoric acid selectively removes silica and enhances visibility of the fossil organic cement.

Experimental maturation of Recent and fossil foraminifers through anoxic pyrolysis indicates that agglutinated foraminifers darken with increasing temperature. Pyrolysis in the presence of oxygen had the effect of lightening fossil colour. Pyrolysis in the presence of petroleum produced different colouration effects than exist in the fossil record. The results from pyrolysis and the fact that foraminiferal colour is independent of associated rock colour indicate that colouration is a primary effect from geothermal maturation and a potential index of maturity.

The Beaufort–Mackenzie Basin contains a dozen or more kilometres of sedimentary section that show the progressive effects of burial diagenesis. Exploration drilling penetrates sections of more or less continual sedimentation as thick as 5 km. Higher levels of diagenesis are present in areas that have undergone as much as 5 to 7 km of erosion. Four zones of burial diagenesis have been recognized in these rocks. Zone A, from burial depths up to 2400 m and temperatures of about 75°C, shows little diagenetic effect in fossil foraminifers. Zone B, from 2400–3500 m and temperatures of about 75–110°C, shows the first sign of burial diagenesis with the occurrence of minor amounts of secondary quartz in the foraminiferal test and a slight darkening of the organic cement. Zone C, from 3500–5000 m and temperatures of about 110–140°C, is characterized by pervasive secondary quartz, resulting in silicification of the foraminiferal test. Zone C is also characterized by clay mineralization, in the form of smectite and kaolin, as well as a further darkening of the test through organic maturation of the foraminiferal cement. Zone D, from burial depths of about 6 to 8 km and temperatures of about 150–250°C, shows complete silicification of arenaceous foraminifers with some precipitation of illitic clay in the interstices. Calcareous-walled foraminifers in Zone D are typically recrystallized and partially replaced by iron or magnesium calcite, or more commonly by chloritic clay. In sediments with high levels of marine organic material, Zone D specimens characteristically become coated with dark bitumen.

An assessment of FCI in six Beaufort–Mackenzie Basin exploration wells indicates that foraminiferal colour shows a linear increase with increasing temperature and depth in wells that have a simple depositional burial history and are normally compacted. Wells that have significant overpressured zones, however, show that the trend of increasing FCI is significantly reduced or even reversed through the overpressured section. Hydrothermal effects from trapped pore waters in these overpressured zones may be responsible for retarding FCI trends. Although overpressuring

may interfere with FCI as a thermal maturation indicator, it does mean that FCI is a potential tool for recognizing overpressured zones.

Foraminiferal colour change seems to depend on heating rate as well as maximum temperature, but it is not possible to develop a kinetic model for this process until the potential complicating effects of overpressure are better understood. Therefore, in this study, FCI values are broadly correlated with temperature for offshore sequences that are believed to be currently at their maximum burial depth. Future work is necessary to determine the relative importance of time, temperature, and pressure to the process of foraminiferal colour change.

Sommaire

Deux nouveaux systèmes d'évaluation de la maturité thermique sont décrits dans le présent bulletin. Le premier est appelé «indice de coloration des foraminifères» (ICF) et repose sur les changements de couleur dus à la chaleur dans le ciment organique des foraminifères à test agglutinant. Le deuxième est basé sur la zonalité de la diagenèse par enfouissement, laquelle est fonction des changements minéralogiques généralisés chez les foraminifères en raison de facteurs géothermiques et hydrothermaux. Ces facteurs sont, entre autres, la précipitation de quartz secondaire (excroissance), la précipitation de minéraux argileux (comme la smectite, la kaolinite, l'illite et la chlorite) ainsi que la recristallisation et le remplacement de la calcite.

La comparaison de données sur l'ICF à des données sur le pouvoir réflecteur de la vitrinite et à des données de pyrolyse Rock-Eval fait ressortir que la couleur des foraminifères est plus sensible aux changements durant les premiers stades de la genèse du pétrole. La silicification des tests de foraminifères commence également à ce stade, de sorte la préservation de ces microfossiles est une indication facile à déceler permettant de déterminer quand les hydrocarbures ont commencé à se former.

Dans le bassin de Beaufort-Mackenzie, les foraminifères sont abondants dans les roches sédimentaires marines et terrigènes du Mésozoïque et du Cénozoïque. Les données sur les fossiles indiquent clairement que les foraminifères subissent des changements progressifs de couleur et de composition minérale à mesure qu'augmente la maturité thermique. Les changements de couleur, qui vont du blanc à des teintes de brun ambré grisâtre à noir, sont dus à la maturation thermique du ciment organique (glycosaminoglycane) qui entoure chaque grain dans le test agglutinant et peut revêtir les surfaces intérieure et extérieure du test entier. La préservation du ciment organique des fossiles est corroborée par des observations au microscope électronique à balayage. Une attaque à l'acide fluorhydrique du test des foraminifères élimine sélectivement la silice et accroît la visibilité du ciment organique fossile.

La maturation expérimentale des foraminifères holocènes et fossiles par pyrolyse anoxique indique que les foraminifères à test agglutinant deviennent plus foncés à mesure que la température augmente. La pyrolyse en présence d'oxygène a eu pour effet d'éclaircir la couleur des fossiles. La pyrolyse en présence de pétrole a produit des couleurs différentes de celles qui existent dans les fossiles. Les résultats obtenus par pyrolyse et le fait que la couleur des foraminifères ne dépend pas de la couleur de la roche associée indiquent que la coloration des microfossiles dérive principalment de la maturation géothermique et s'avère un indicateur potentiel de la maturité des matériaux.

Le bassin de Beaufort-Mackenzie contient au moins une douzaine de kilomètres d'épaisseur de roches sédimentaires qui affichent les effets graduels de la diagenèse par enfouissement. Des puits d'exploration pénètrent des empilements mesurant jusqu'à 5 km d'épaisseur où la sédimentation a été plus ou moins continue. Une diagenèse plus marquée s'observe dans les zones où l'érosion a enlevé 5 à 7 km de matériel. Quatre zones de diagenèse par enfouissement ont été identifiées dans ces roches. La zone A, dont les profondeurs d'enfouissement atteignent 2 400 m et les températures environ 75 °C, présente peu d'indices de diagenèse dans les foraminifères fossiles. La zone B, avec

des profondeurs d'enfouissement de 2 400 à 3 500 m et des températures de 75 à 110 °C, affiche les premiers signes de diagenèse par enfouissement, soit la présence de faibles quantités de quartz secondaire dans le test des foraminifères et un léger assombrissement de la couleur du ciment organique. La zone C, située entre 3 500 et 5 000 m de profondeur et dont les températures varient entre 110 et 140 °C, se caractérise par l'omniprésence de quartz secondaire résultant de la silicification des tests des foraminifères. La zone C se reconnaît aussi à l'altération en argile, sous la forme de smectite et de kaolinite, ainsi qu'à un assombrissement plus prononcée du test par maturation organique du ciment des foraminifères. Dans la zone D, enfouie sous environ 6 à 8 km de roches à des températures variant entre 150 et 250 °C, la silicification des foraminifères arénacés est complète et accompagnée de la précipitation plus ou moins abondante d'illite dans les interstices. Les foraminifères à parois calcaires de la zone D sont habituellement recristallisés et partiellement remplacés par de la calcite ferrifère ou magnésienne ou, le plus souvent, par de la chlorite. Dans les roches sédimentaires contenant des concentrations élevées de matières organiques marines, les spécimens de la zone D sont typiquement revêtus de bitume foncé.

Une évaluation de l'ICF dans six puits d'exploration forés dans le bassin de Beaufort-Mackenzie révèle que, dans ceux où l'enfouissement est historiquement simple et où la compaction est normale, la couleur des foraminifères s'assombrit de façon linéaire avec la hausse de la température et l'augmentation de la profondeur. On observe cependant que, dans les puits traversant des zones en surpression d'importance, la tendance à la hausse de l'ICF diminue significativement ou même s'inverse dans la section en surpression. Les effets hydrothermaux dus au piégeage des eaux interstitielles dans ces zones en surpression peuvent être à l'origine de ces changements quant à l'évolution de l'ICF. Même si dans les zones de surpression, l'utilisation de l'ICF comme indicateur de maturation thermique est incertaine, il n'en demeure pas moins qu'il s'avère un outil potentiel pour la localisation des zones en surpression.

Le changement de couleur des foraminifères semble dépendre du taux d'augmentation et de la valeur maximale de la température; il n'est cependant pas possible d'élaborer un modèle cinétique de ce processus aussi longtemps que les effets potentiels complexes de la surpression n'auront pas été compris. Ainsi, dans la présente étude, les indices de coloration des foraminifères sont généralement corrélés à la température des séquences extracôtières qui sont censées avoir atteint leur profondeur d'enfouissement maximale. Des travaux supplémentaires seront nécessaires pour déterminer l'importance relative du temps, de la température et de la pression dans le processus de changement de couleur observé dans les foraminifères.

INTRODUCTION

The study of organic thermal alteration has focused traditionally on primary coaly macerals, such as vitrinite and alginite, structureless material such as sapropelic groundmasses and bituminite, and the actual hydrocarbon end products (Robert, 1985). Studies on mineralogical changes induced through burial diagenesis of terrigenous clastic rocks have focused on silica, feldspar, carbonates, and mineral cements such as silica and calcite and, in the finer fractions, on the clay minerals such as smectite, illite, kaolinite, and chlorite (Chilingarian and Wolf, 1988). Thermal maturation has also been assessed paleontologically, from pollen, spores, and organic matter (Staplin, 1969), chitinozoa (Goodarzi, 1985), conodonts (Epstein et al., 1977; Rejebian, 1987), ostracods (Ainsworth et al., 1990), graptolites (Goodarzi and Norford, 1989), and scolecodonts (Goodarzi and Higgins, 1987).

Foraminifers were introduced as potential indices of geothermal maturity by McNeil et al. (1989, 1990), who recognized colouration changes in foraminiferal organic cement and in the silicification of the foraminiferal test. Similar features were interpreted differently by Alabusheva (1990), who saw the colouration of foraminifers resulting secondarily from colouration by associated geothermally maturing humin. Rosen (1991) introduced a colour alteration index based on colour trends in agglutinated foraminifers from Tertiary clastic sediments in the Gulf of Mexico. Six colour grades were recognized as representing progressive thermal alteration of the organic cement of the agglutinated foraminifers (amber, amber brown, brown, grey, black, and white). The attainment of white colouration was interpreted as the volatilization of whatever compound was responsible for the initial colouration trends.

Little has been done to document the mineralogical changes which occur during burial diagenesis of foraminifers, either agglutinated or calcareous. Reiser (1988), however, recognized that the conversion of aragonite to calcite in the foraminiferal family Robertinacea could be used as an indicator of thermal maturity.

In this paper, we introduce a scheme referred to as FCI (Foraminiferal Colouration Index) for quantifying colour change in agglutinated foraminifers. Additionally, we document a generalized sequence of diagenetic changes involving silica, kaolin, smectite, illite, and chlorite in foraminifers. All observations and conclusions have been established from the foraminiferal record in the Mesozoic–Cenozoic Beaufort–Mackenzie Basin of arctic Canada. Both FCI and the burial diagenesis zonation were empirically established from successive changes in the fossil record in rocks of increasing thermal maturity. For comparative purposes, thermal maturity trends were established independently by vitrinite reflectance measurements and Rock-Eval analysis.

Agglutinated foraminifers are widespread in terrigenous clastic sedimentary basins. In the Beaufort–Mackenzie Basin, for example, they inhabit virtually every marine facies from the shoreline to the deep sea. They are particularly common in shallow-water facies, in deltaic facies, and in deep-water facies. The Beaufort–Mackenzie Basin contains a full spectrum of sedimentary facies, has a wide range of agglutinated foraminiferal assemblages from a wide variety of ages, rock types, and maturity levels and is therefore ideally suited for the study documented herein.

ACKNOWLEDGMENTS

We gratefully acknowledge the technical assistance of C.J. Klep (FCI data collection), R.G. Fanjoy (Rock-Eval analysis), J.N.Y. Wong (SEM and EDX analysis), and D.R. Then (drafting). The constructive comments of critical reviewers D.W. Morrow and J. Utting also are gratefully acknowledged. The initial stages of this research project benefited from technical guidance and moral encouragement received from F. Goodarzi (organic petrology) and A.E. Foscolos (clay mineralogy).

ORGANIC MATTER IN THE FORAMINIFERAL TEST

Foraminifers are marine protozoans that construct a test around a single cell. The test may be quite varied in morphology but generally consists of tubular, globular, or wedge-shaped chambers in a variety of arrangements (Fig. 1). Foraminifers can be broadly divided into two groups, one constructed by agglutinated detrital grains, the other constructed by secreted calcite. Although mineralogically different, both forms utilize organic matter in the construction of their test.

The agglutinated foraminiferal test typically has two basic elements, detrital grains and organic cement, both of which are commonly fossilized. The detrital grains (Fig. 2) which form the main bulk of the test are potentially diverse, but in siliciclastic sediments the majority are grains of quartz. Quartz grains range in size from several microns to a tenth of a millimetre or more. The organic cement (Fig. 2) consists mostly of glycosaminoglycans (=mucopolysaccharides) which are unbranched polysaccharide chains of proteoglycans composed of repeating disaccharide sequences of amino sugars (Langer, 1992). The organic cement has numerous organizational characteristics, and its physical distribution has been documented in great detail (Bender, 1989). It may occur as a thin lining on the test exterior and interior, as well as around individual grains. It also occurs within the wall, between grains in three basic patterns: as single strands, as a fibrous meshwork, or as a spongy matrix (Bender and Hemleben, 1988; Bender, 1989). Organic cement is thus distributed throughout most of the test, although the most visible organic structure is usually the inner lining.

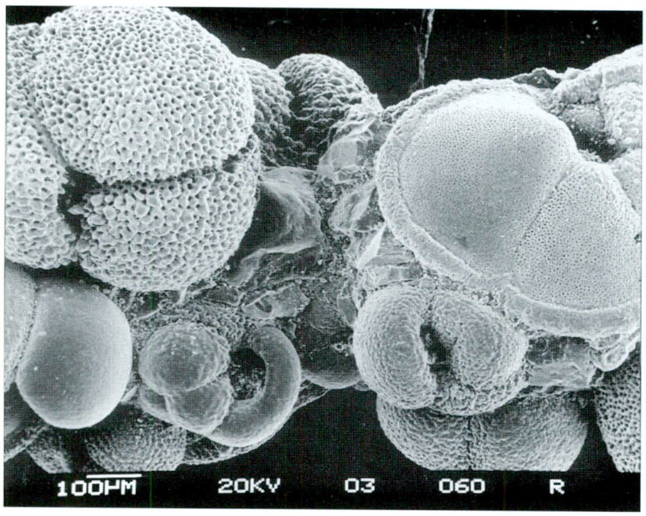

*Figure 1. Planktonic foraminifers agglutinated to the arenaceous test of **Rhabdammina**, GSC 112227. From deep-sea planktonic ooze, Baltimore Canyon, North Atlantic Ocean.*

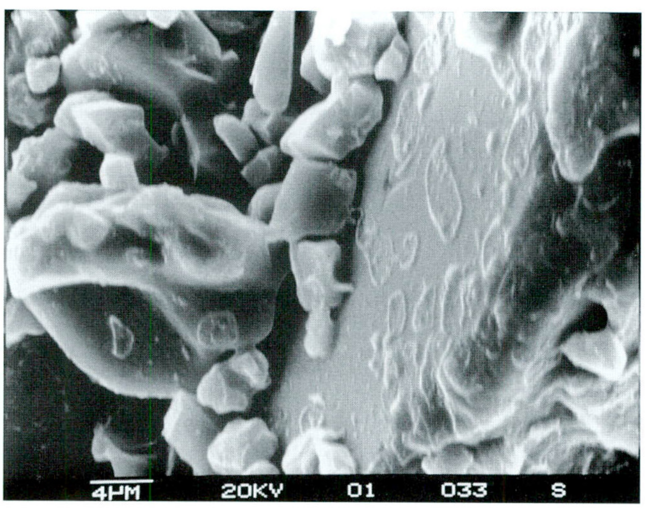

*Figure 2. Detail of agglutinated grains in the wall of Holocene **Rhabdammina**, GSC 112228. Organic cement (glycosaminoglycans) coats each grain.*

The calcareous (secreted) foraminifers may possess organic matter in the form of inner and outer organic linings composed of proteins and polysaccharides (Weiner and Erez, 1984). In addition, the pores that are present in the majority of calcareous species can be lined by an organic wall and partitioned by organic sieve plates. In foraminifers where test growth leads to successive layering of calcite, organic layers may occur between calcite layers (Hemleben et al., 1988, p. 196, 197).

In this study, we focus primarily on the agglutinated foraminifer because the pervasive distribution of organic cement throughout the organism provides greater potential for the recognition of thermal alteration and for the practical reason that they are very abundant in the Beaufort-Mackenzie Basin. We have also observed, as will be illustrated later, that the agglutinated test sensitively reflects increasing levels of thermal maturity by progressively darker colouration. Colouration in the calcareous foraminifers has been observed to differ from associated agglutinated foraminifers and to be more a reflection of the presence or absence of oxidized iron in the calcareous wall. This does not preclude calcareous foraminifers from being utilized as indices of maturation. The organic linings of foraminifers and the organic layers found within the calcite wall may have some potential use in maturation studies, but these avenues are not pursued in the current study.

SAMPLES

Geochemical, mineralogical, and geothermal data for this study have been collected primarily from seven exploration wells penetrating Jurassic to Cenozoic strata in the Beaufort-Mackenzie Basin of northwestern arctic Canada (Figs. 3, 4). Four of the wells (Amerk O-09, Amauligak J-44, Arluk E-90, and Issungnak 2O-61) are located offshore in the basin depocentre where sediments reach thicknesses of 12 km or more. The upper 4 or 5 km of this section is currently undergoing compaction and has a relatively low geothermal gradient. The present day 100°C isotherm is slightly less than 4 km deep (Hitchon et al., 1990) and the thermal maturity of sediments in these wells reaches a maximum vitrinite reflectance of about 0.55%Ro. Onshore, the Reindeer D-27 and Wagnark G-12 wells, situated in the Kugmallit Trough, penetrate Paleogene and Upper Cretaceous strata, with vitrinite reflectance values of 0.29 to 0.60%Ro (Reindeer D-27). To the west, on the Yukon Coastal Plain, much higher

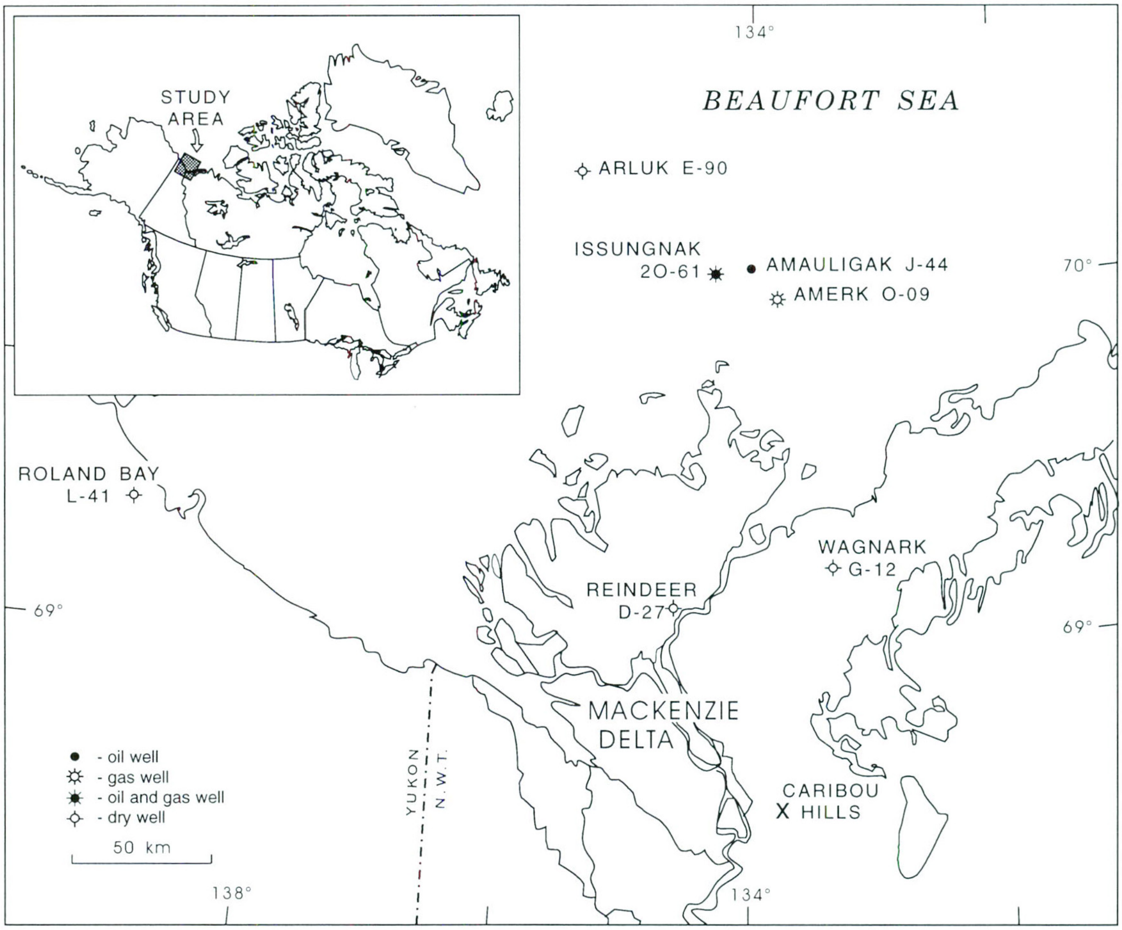

Figure 3. Map of study area, well and outcrop locations.

levels of thermal maturity, ranging from 2.0 to 4.3%Ro, were encountered in Cretaceous and Upper Jurassic strata of the Roland Bay L-41 well. Rocks of Paleocene and Late Cretaceous age outcropping in the vicinity of the Caribou Hills, were also analysed and are representative of older rocks that have undergone low levels of maturation.

OBSERVATIONS AND HYPOTHESES

Observation of the preservation of fossil foraminifers from Jurassic to Cenozoic strata of the Beaufort–Mackenzie Basin and environs has revealed three conspicuous trends: 1) the colour of fossil agglutinated foraminifers darkens progressively with increasing levels of thermal maturity (Fig. 5); 2) the texture and mineralogy of the agglutinated wall changes with increasing levels of thermal maturity, from a loosely aggregated granular arrangement of quartz grains to a less-porous, crystalline (silicified) texture (Fig. 6), with minor amounts of authigenic kaolin, smectite, and illite; 3) calcareous foraminiferal tests are recrystallized and chlorite replaces calcite at high levels of thermal

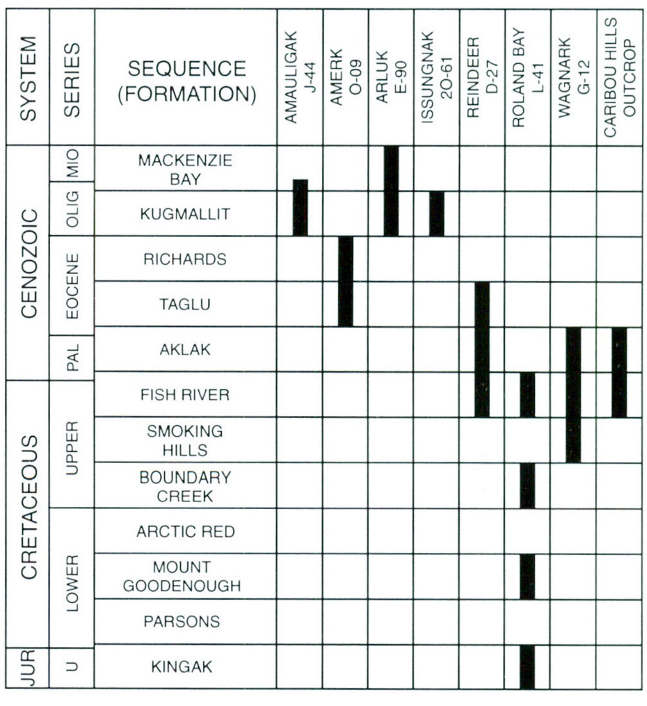

Figure 4. Stratigraphic units of the Beaufort–Mackenzie Basin and sample distribution.

maturity (Fig. 7). To explain these trends three hypotheses are proposed: 1) the changes in colour are caused by thermal alteration of the organic cement that is pervasive throughout agglutinated foraminifers, 2) the silicification of the agglutinated test is caused by thermally controlled precipitation of silica and clay minerals from SiO_2-saturated pore fluids in argillaceous rocks, and 3) foraminiferal calcite is unstable at high geotemperatures and is recrystallized and replaced by authigenic chlorite.

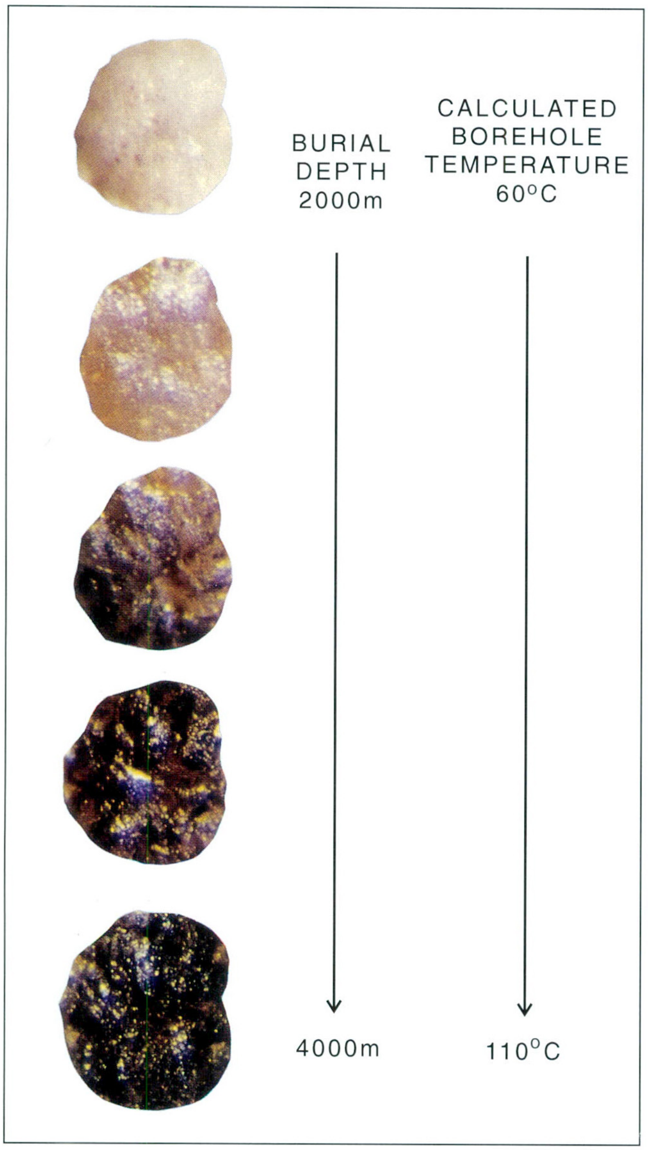

Figure 5. Typical colour sequence recognized in fossil foraminifers from the Beaufort-Mackenzie Basin, arctic Canada. Specimens GSC 112229–112233 from the Amauligak J-44 well, see also Figure 9.

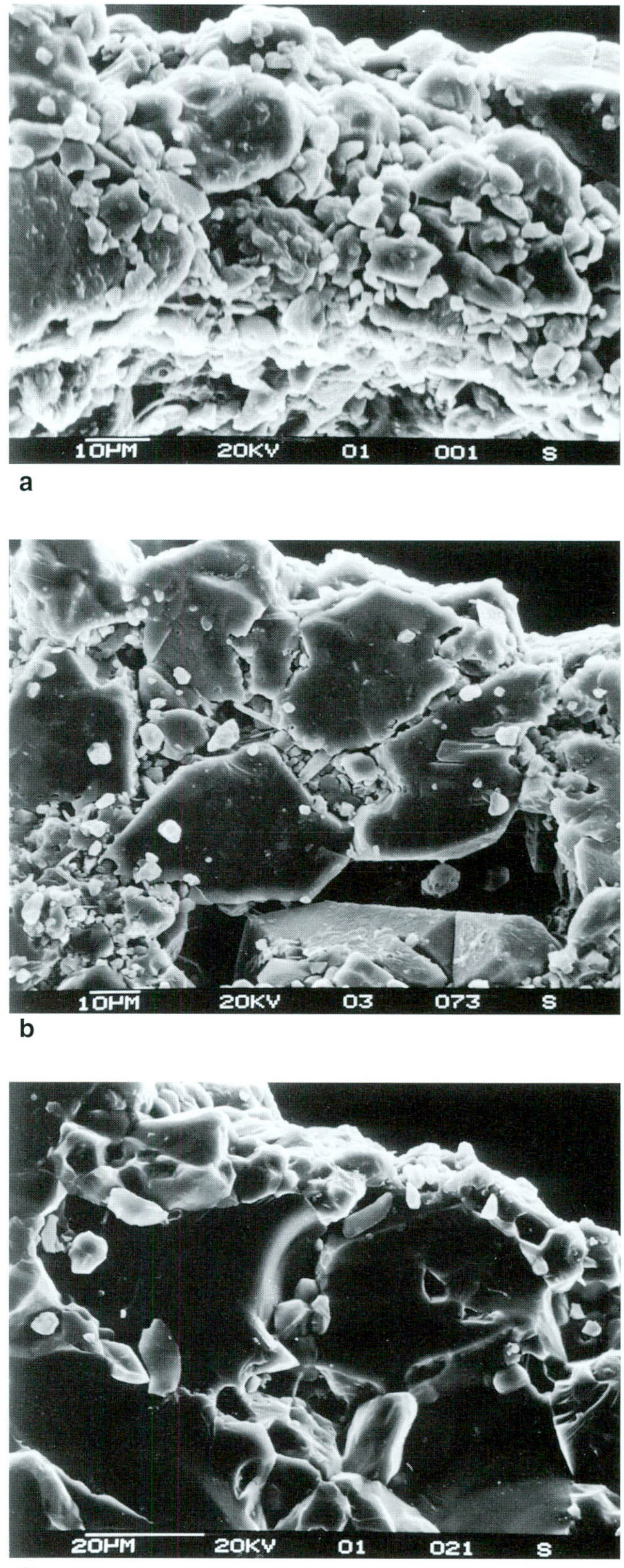

fig_6.ai

Figure 6. Micrographs showing progressive alteration of the test wall of agglutinated foraminifers by secondary development of quartz (silicification) with increasing burial diagenesis. ***a. Recurvoides****, GSC 112234, Recent. Cross-section of test wall showing unaltered agglutinated grains;* ***b. Reticulophragmium****, GSC 112235, Oligocene, present burial depth 4115 m. Cross-section showing alteration of agglutinated test wall by secondary quartz overgrowths (silicification);* ***c. Haplophragmoides****?, GSC 112236, Late Jurassic, estimated maximum paleoburial depth 6 to 8 km. Cross-section of fully silicified test wall of an agglutinated foraminifer.*

QUANTIFICATION OF COLOUR ALTERATION

Foraminiferal colour alteration can be quantified fairly accurately by visual comparison of fossil colour with the standard colour sequence illustrated in the Munsell Soil Colour Chart (1975). Colours are categorized by value (white to black), hue (primary colour), and chroma (saturation). Foraminiferal colours in the Beaufort–Mackenzie Basin are illustrated in Figure 8 and show a full range of values from white to black, relatively unsaturated or greyish chromas, and hues of greyish brown. For the purpose of determining maturation level, the value (or darkness) of the fossil colour is the most significant of the three parameters in the Munsell Colour Chart. The practical assessment of value is done by placing specimens on standard Munsell colour chips for direct comparison. The value is then converted directly into an FCI number as indicated in Table 1. Foraminiferal specimens and their corresponding FCI numbers are illustrated in Figure 8. Each foraminifer will undoubtedly show some internal or external variation in colour, depending on quantity and type of original organic matter, but it is the overall colour of the test wall that is used to make the numerical assessment. Specific parts of the test, such as the inner organic lining will be much darker than the overall colour of the agglutinated wall and are not used in this scheme. Specimens which fall between two values on the Munsell Colour Chart could be assigned to the mid-point between those values. Using these half step values, a greater precision is attainable from the chart.

Recent agglutinated foraminifers (FCI 0) are commonly coloured rusty brown (Fig. 8). The rusty brown colouration is imparted by trace amounts of iron which is oxidized at or near the surface of the marine substrate. With burial, the iron oxide is reduced and possibly leached (Sidner and McKee, 1975, 1976). The fossil test is transformed to a white colour and remains so at low levels of thermal maturation. In the Beaufort–Mackenzie Basin, virtually all fossil agglutinated foraminifers examined at low levels of thermal maturation are white and these are assigned to FCI 1 (Fig. 8).

The recovery of abundant agglutinated foraminifers from thick terrigenous clastic sequences in the Beaufort–Mackenzie Basin has provided an ideal section from which to observe and document further changes in the colour of fossil agglutinated foraminifers. The Amauligak J-44 discovery well has been chosen as a representative example to document maturation trends (Fig. 9) which occur in wells throughout the basin. This sequence of changes is of particular importance since it illustrates thermal conditions that correspond to the early stages of hydrocarbon generation. Vitrinite reflectance data and Rock-Eval pyrolysis have been used to assess the level of thermal maturity of this section. Issler and Snowdon (1990) have modelled the thermal history of the Amauligak J-44 well using kinetic parameters for hydrocarbon generation and concluded that the well penetrated only low maturity sediments.

The progressive colouration of agglutinated foraminifers in the Amauligak J-44 well from white to dark amber correlates with increasing vitrinite reflectance values that range from 0.32 to 0.56%Ro. Rock-Eval (Tmax) results over the same section increase from 418° to 427°C (Fig. 9).

The sequence of fossil colours that is illustrated in Figure 9 is based on specimens from a single species, *Labrospira turbidus*. The FCI histograms, however, were tabulated from the entire fossil population recovered from well cuttings samples from the indicated intervals. In this particular well, the fossil assemblage includes specimens from tubular foraminifers such as *Bathysiphon* and *Rhabdammina*, and more complex forms such as *Haplophragmoides*, *Labrospira, Recurvoides*, and *Reticulophragmium*. The colour is notably darker in specimens that have inner organic linings preserved, but as stated earlier, only the general colour of the test wall is used in determining FCI. The section at Amauligak J-44 has FCI levels of 1 to 6 and Munsell colours of 10YR8/1 to 10YR4 (white to dark greyish brown). Colour of the associated shales and sandstones shows no relationship with foraminiferal colouration. Colour of the rocks through the section illustrated in Figure 9 ranges from light olive grey at 2200 m to olive grey at 4000 m.

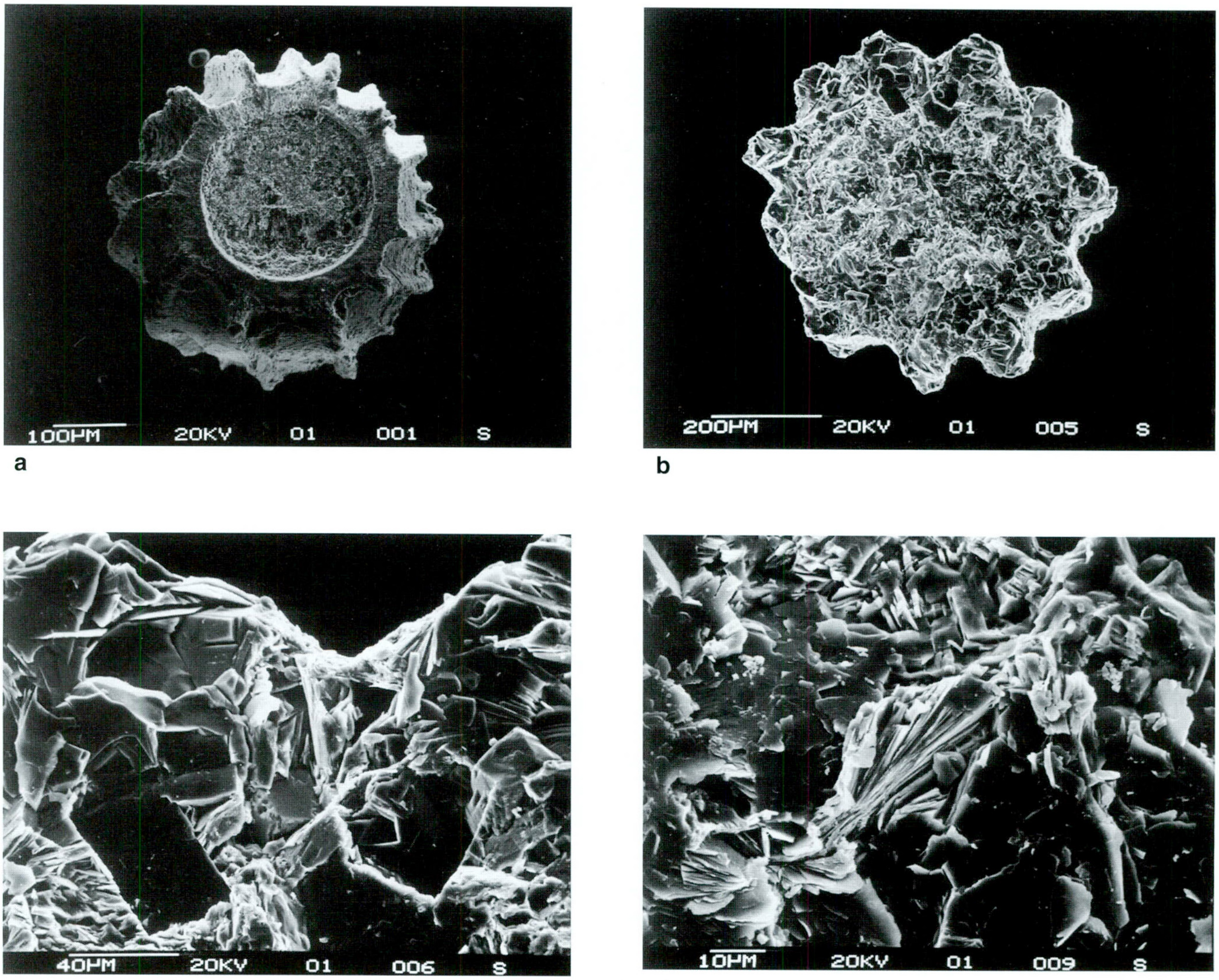

Figure 7. Micrographs showing alteration of the test wall of calcareous foraminifers through recrystallization and chloritization with increasing burial diagenesis. ***a.*** *Nodosarid, GSC 112237, Eocene. Cross-section of test wall showing little or no alteration;* ***b. Marginulina****, GSC 112238, Late Jurassic. Estimated maximum paleoburial depth 6 to 8 km. Cross-section of altered test wall showing recrystallized calcite in a matrix of secondary chlorite;* ***c.*** *Detailed cross-section of* ***Marginulina*** *(from 7b) showing recrystallized test wall, calcite rhombs, and chlorite filling the test interior;* ***d.*** *Detail of the interior of* ***Marginulina*** *(from 7b) showing bladed secondary chlorite filling the test along with recrystallized calcite.*

Statistical assessment of foraminiferal colouration can be achieved by tabulation of measurements on the entire assemblage in a sample. Measurements on a number of specimens will produce a range of values, as illustrated in the histograms in Figure 9. An average FCI value can be calculated, but in the case of well cuttings a closer assessment of the data might be necessary. A bimodal histogram could differentiate, fairly definitively, between in situ and caved material. The caved material can be eliminated from the calculation of FCI. Similarly, reworked specimens derived from hotter geothermal regimes could be recognized and eliminated.

In many areas, practical necessities dictate that most data will be derived from well cuttings. Ideally, however, FCI measurements would be derived from core or unweathered outcrop samples. FCI data from core in the Issungnak 2O-61 well (Fig. 10) provides a good illustration of the range of FCI values to be expected from a typical assemblage dominated by *Labrospira* sp. In most histograms the mode is fairly well differentiated and the calculated average always lies within the mode. In any one sample, the range of values is typically spread over three increments on the FCI scale, rarely four, and a normal or slightly skewed distribution of data is apparent in all the samples.

The present day geothermal gradients in the Beaufort-Mackenzie Basin are relatively low, ranging from 23 to 33 mK/m (Majorowicz and Dietrich, 1989). The geothermal maturation gradient in the Beaufort-Mackenzie Basin is also known to be relatively low (Issler and Snowdon, 1990) and this is largely a result of rapid sedimentation/burial rates in the basin. Wells commonly penetrate up to a depth of 5 km and do not exceed a maturity level of about 0.50 to 0.60%Ro. Corresponding average FCI values do not exceed 5.5 to 6.0. Specimens from a higher geothermal regime were obtained from the Roland Bay L-41 well, situated a short distance to the west of the Beaufort-Mackenzie Basin. Regional erosion at the L-41 site has exposed Lower Cretaceous rocks overlying the Jurassic. Vitrinite reflectance measurements from this section increase downhole from about 1.9 to 4.3%Ro near the well's total depth. Histograms showing FCI data through the L-41 well are shown in Figure 11. Average FCI values in the Roland Bay L-41 well range from 5.73 at 122 m to 10 at 2195 m. Data from the Roland Bay L-41 well indicate that there is little change in FCI at maturation levels between 2.40 and 4.30%Ro.

Table 1

Foraminiferal Colouration Index (FCI) compared to standard colour sequence from the Munsell Soil Colour Chart. Thermally-altered agglutinated foraminifers typically show colouration changes within the yellow-red (YR) hue. The colours indicated below are from the 10YR soil chart which shows yellowish hues. Standard Munsell colour chips are available for all FCI values except FCI 8 which falls between brownish black and black and therefore must be estimated.

FCI	MUNSELL COLOUR STANDARD	
0	7.5YR6/6	reddish yellow
1	10YR8/1, 10YR8/2	white
2	10YR7/1, 10YR7/2	light grey
3	10YR6/1, 10YR6/2	light brownish grey to grey
4	10YR5/1, 10YR5/2	grey to greyish brown
5	10YR4/1, 10YR4/2	dark grey to dark greyish brown
6	10YR3/1, 10YR3/2	very dark grey to very dark greyish brown
7	10YR2/1, 10YR2/2	very dark brown to brownish black
8	10YR2/1 – N2/0	very brownish black
9	N2/0	black (partially translucent)
10	N2/0	black (opaque)

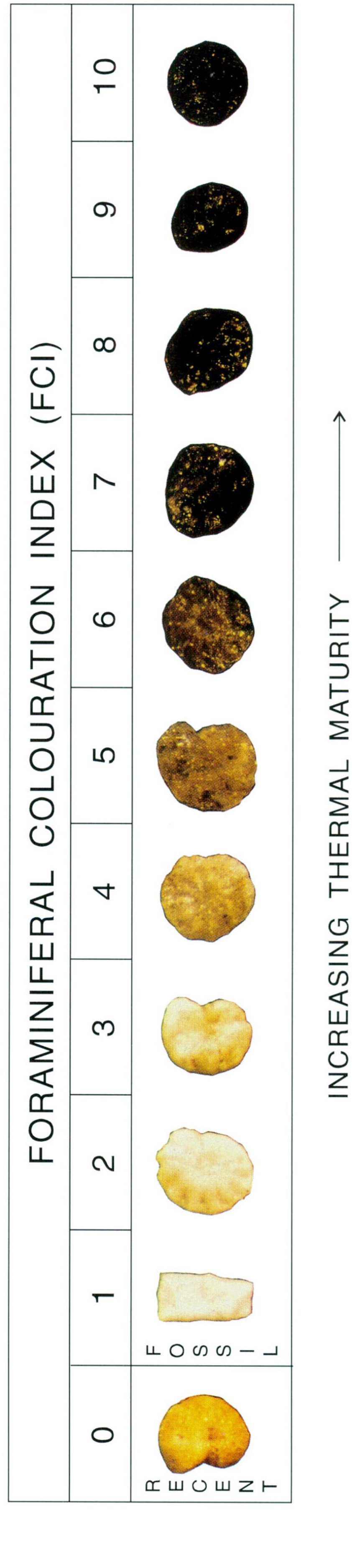

Figure 8. *Foraminiferal Colouration Index (FCI). Left to right, GSC 112239 to 112249.*

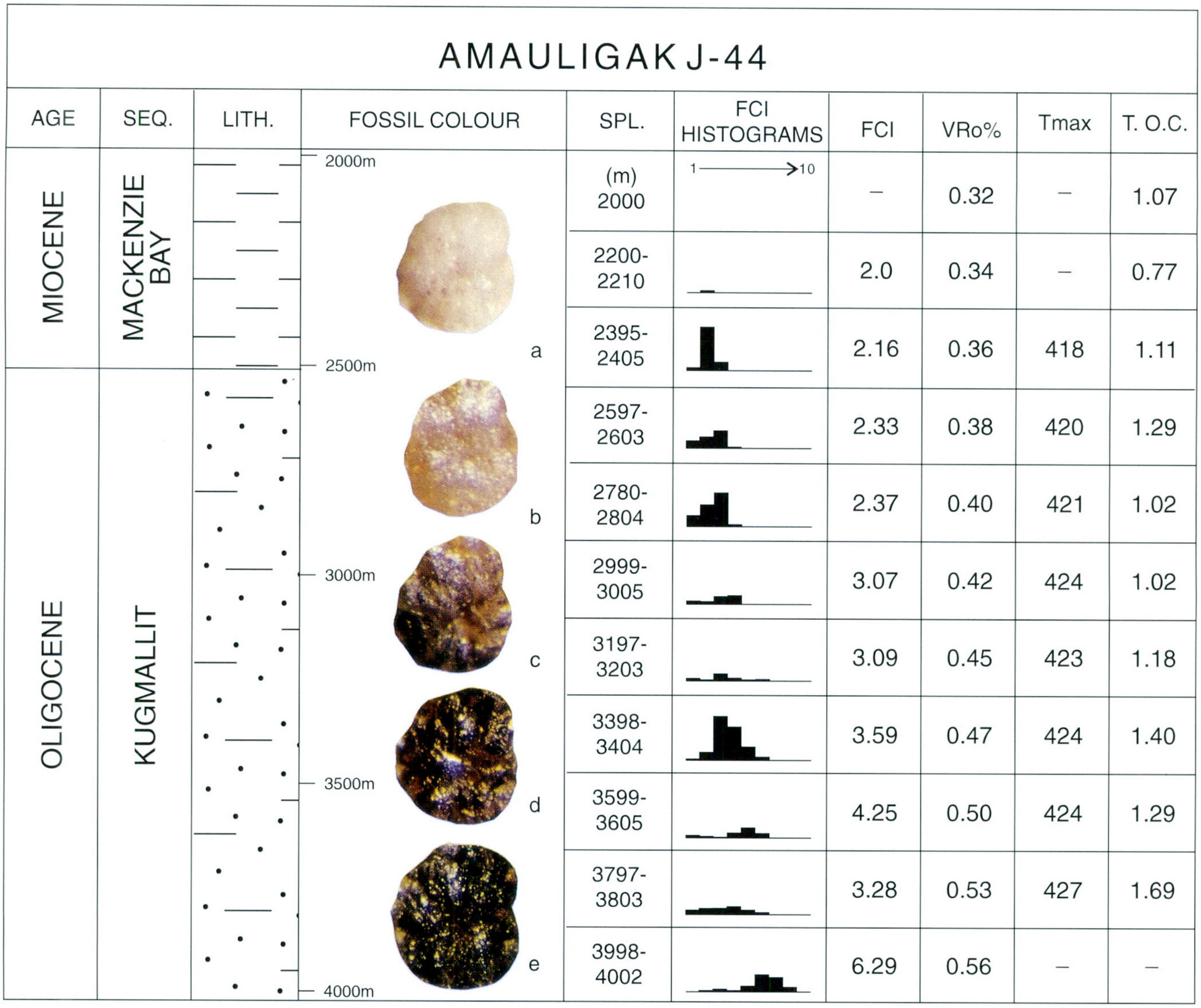

SPL. (m)	FCI	VRo%	Tmax	T. O.C.
2000	–	0.32	–	1.07
2200-2210	2.0	0.34	–	0.77
2395-2405	2.16	0.36	418	1.11
2597-2603	2.33	0.38	420	1.29
2780-2804	2.37	0.40	421	1.02
2999-3005	3.07	0.42	424	1.02
3197-3203	3.09	0.45	423	1.18
3398-3404	3.59	0.47	424	1.40
3599-3605	4.25	0.50	424	1.29
3797-3803	3.28	0.53	427	1.69
3998-4002	6.29	0.56	–	–

Figure 9*. Thermal maturity indices (FCI, VRo, Tmax) and total organic carbon measured from cuttings samples in the Amauligak J-44 well, central Beaufort Sea. Vitrinite reflectance values were estimated from measurements on samples from the Amauligak F-24 well (P. Mukhopadhyay, pers. comm., 1991) situated several kilometres to the east.* ***a. Haplophragmoides****, GSC 112229;* ***b. Haplophragmoides****, GSC 112230;* ***c. Labrospira****, GSC 112231;* ***d. Labrospira****, GSC 112232;* ***e. Labrospira****, GSC 112233.*

EXPERIMENTAL VERSUS GEOTHERMAL COLOUR ALTERATION

In an attempt to establish an experimental basis for thermal alteration of the agglutinated test, Recent and fossil specimens of foraminifers were pyrolyzed in the laboratory. Experiments were conducted in the absence of water at temperatures of 310°C, 320°C, and 330°C. Initial heating experiments were conducted under an inert He atmosphere at 95 bars of pressure for 72 hours. For comparative purposes, pyrolysis experiments were also run with specimens exposed to air at atmospheric pressure. A final pyrolysis experiment was carried out on specimens that had been saturated with crude oil.

In the initial experiment, Recent and fossil specimens of foraminifers (agglutinated, calcareous benthic and planktonic), Recent ostracods, and conodonts were heated. Pyrolysis produced at least slight darkening in all specimens (compare Figs. 12 and 13). Striking colour change occurred only in Recent specimens of *Rhabdammina* and *Recurvoides*, and to some extent in fossil *Cibicidoides*. All of these foraminifers had at least one thing in common, their original colour was red, indicating the presence of

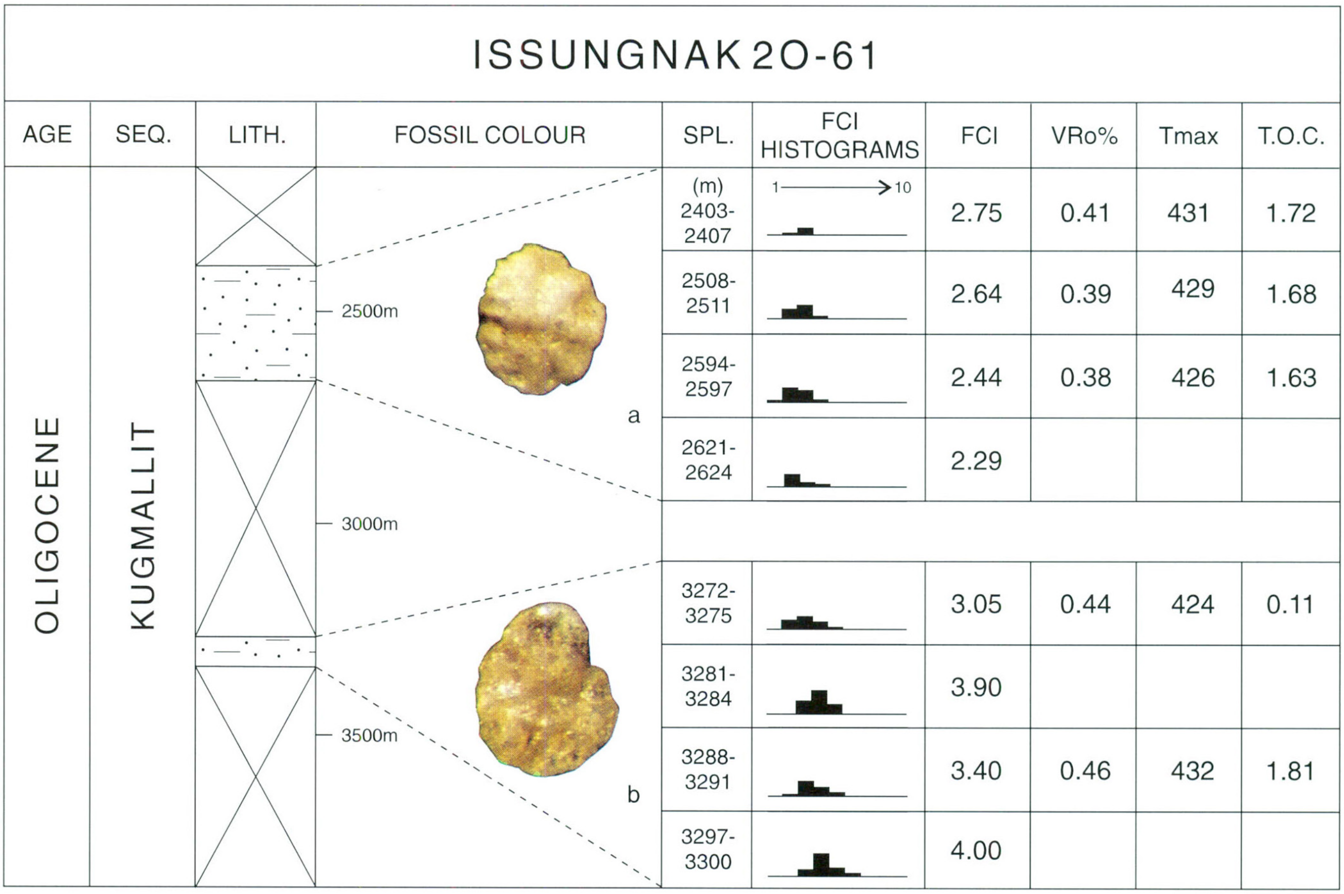

SPL. (m)	FCI HISTOGRAMS	FCI	VRo%	Tmax	T.O.C.
2403-2407		2.75	0.41	431	1.72
2508-2511		2.64	0.39	429	1.68
2594-2597		2.44	0.38	426	1.63
2621-2624		2.29			
3272-3275		3.05	0.44	424	0.11
3281-3284		3.90			
3288-3291		3.40	0.46	432	1.81
3297-3300		4.00			

***Figure 10**. Thermal maturity indices (FCI, VRo, Tmax) and total organic carbon measured from core samples from the Issungnak 2O-61 well, central Beaufort Sea. **a. Haplophragmoides**, GSC 112250; **b. Labrospira**, GSC 112251.*

oxidized iron. In the agglutinated foraminifer, iron is an integral part of the organic cement (Hedley, 1963); in the calcareous benthic foraminifers the distribution and function of iron is not as well understood. Is the iron primary and associated with some form of organic material in the calcareous test, or is it mineralized either primarily or secondarily in the calcite test? Further research on the distribution of organic matter and iron in the calcareous foraminifers may be needed to resolve this question. Observation of colouration of foraminifers in core from the Issungnak 2O-61 well, on the other hand, illustrates that thermally controlled colouration of agglutinated foraminifers is not paralleled by associated iron-bearing calcareous foraminifers.

Little or no change was observed in the other Recent specimens tested, including *Karreriella*, *Sigmoilopsis*, the calcareous foraminifers, and the ostracods, all of which were initially nearly white or ivory coloured. *Karerriella* has a calcareous rather than organic cement and *Sigmoilopsis* apparently contains very little organic cement, a feature that was confirmed using SEM observations.

Fossil foraminifers representing a sequence of increasing maturation levels (Fig. 14) responded to pyrolysis by each becoming slightly darker, overprinting the initial colouration, but not by a factor that would mask the original variations in maturity levels between these specimens. Specimens that contained copious amounts of organic cement, such as *Arenobulimina* and *Recurvoides* from the Wagnark G-12 well, developed the darkest colour. Interestingly, these specimens appeared to literally exude dark organic matter. For comparative purposes, pyrolysis experiments were also performed in the presence of air and in the presence of crude oil (Fig. 15). Similar suites of specimens were heated in the same manner as the previous anoxic experiments. Heating in the presence of air tended to bleach or lighten the colour of all material tested. It was concluded that organic matter had been burnt off, thus whitening the specimens and that these experimental parameters would not produce meaningful results for geothermal maturation.

A final test was conducted with Recent foraminifers and ostracods that had been immersed in crude oil, drained of excess oil, and then heated under an

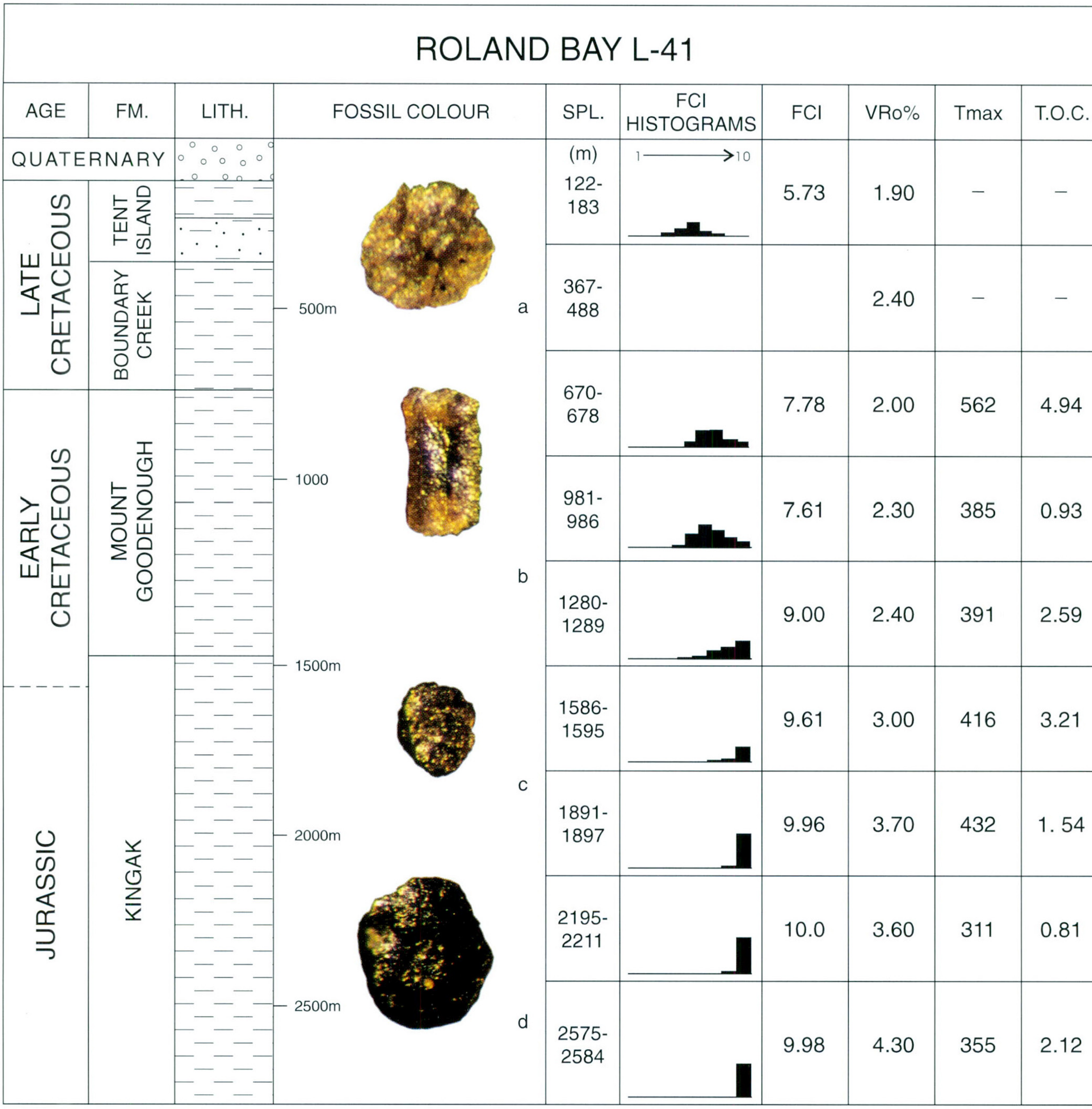

***Figure 11**. Thermal maturity indices (FCI, VRo, Tmax) and total organic carbon measured from core samples from the Roland Bay L-41 well, northern Yukon Territory. **a. Haplophragmoides**, GSC 112252; **b. Bathysiphon**, GSC 112253; **c. Haplophragmoides**, GSC 112254; **d. Haplophragmoides**, GSC 112255.*

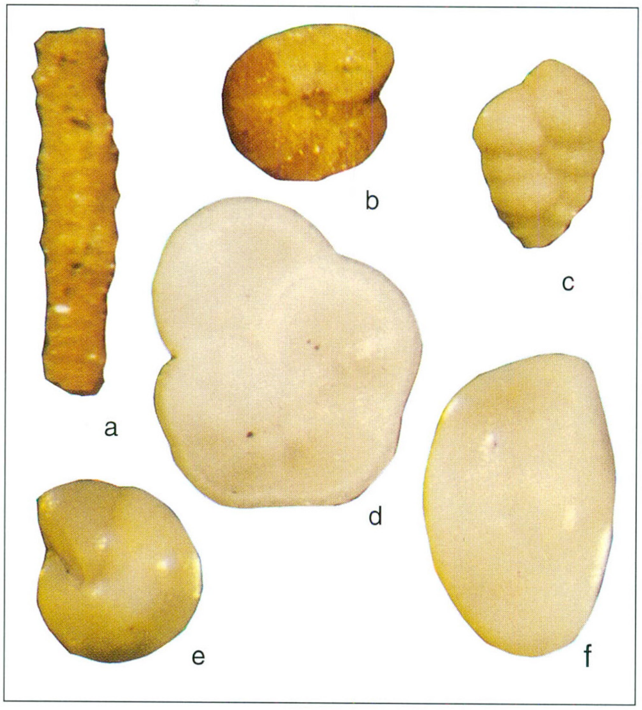

Figure 12. Examples of colour in microfossils.
a. ***Rhabdammina****, GSC 112256, Holocene;*
b. ***Recurvoides****, GSC 112257, Holocene;*
c. ***Karreriella****, GSC 112258, Holocene;*
d. ***Globorotalia****, GSC 112259, Holocene;*
e. ***Cibicidoides****, GSC 112260, Pliocene;*
f. ostracod, GSC 112261, Holocene.

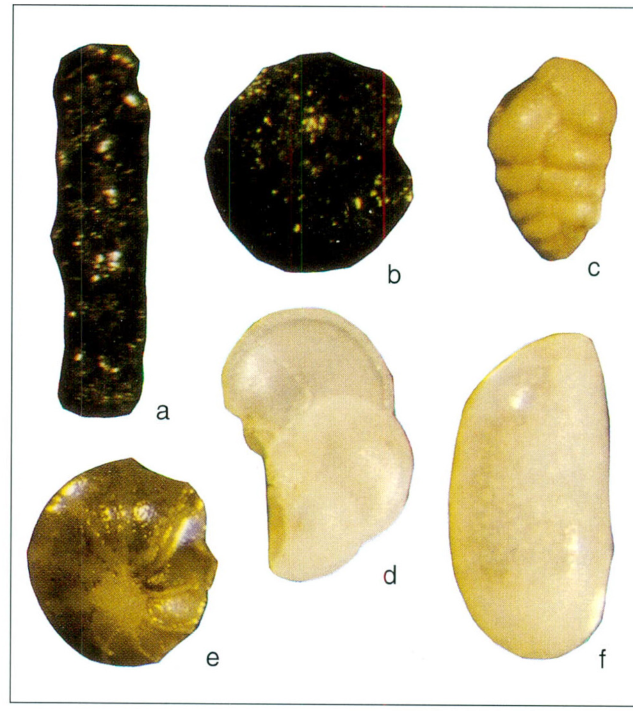

***Figure 13.** Colour alteration effects in microfossils (same taxa as in Fig. 12) after heating by pyrolysis. Effects are greatest for agglutinated specimens (a, b) containing copious amounts of organic cement. Slight darkening effect in **Karreriella** (c) which is agglutinated by calcareous cement. Little or no colouration effect in planktonic foraminifer **Globorotalia** (d) and the ostracod specimen (f). Significant colouration in fossil specimen **Cibicidoides** (e) indicates presence of organic pore linings in test wall. **a. Rhabdammina**, GSC 112262, Holocene; **b. Recurvoides**, GSC 112263, Holocene; **c. Karreriella**, GSC 112264, Holocene; **d. Globorotalia**, GSC 112265, Holocene; **e. Cibicidoides**, GSC 112266, Pliocene; **f.** ostracod, GSC 112267, Holocene.*

anhydrous and anoxic atmosphere (He). This experiment produced darker colouration in all specimens. The agglutinated foraminifers *Recurvoides* and *Rhabdammina* became quite dark, essentially greyish black; *Karreriella* became light brown; the calcareous foraminifers light brown, and the ostracods light brown to dark brown. In the lighter coloured specimens, colouration was darkest in pore spaces and where sediment adhered to the test. Since this contrast in colouration did not match what was found in the fossil record, i.e., colouration in the fossil suites seemed to be independent of adhered clay matrix on specimens, it was concluded that secondary colouration by crude petroleum or some other related hydrocarbon could not be used to explain foraminiferal colouration.

The conclusions from these pyrolysis experiments are not entirely unequivocal, but the following have been drawn. The organic cement of Recent foraminifers becomes much darker after pyrolysis and indicates that it is potentially the origin of colour change due to geothermal effects. Specimens with little or no cement showed little or no darkening after pyrolysis. The presence or absence of iron is a factor in colour change by pyrolysis and this may overwhelm the colour of Recent foraminifers subjected to pyrolysis, but observation of fossil material suggests that iron is not involved in progressive fossil darkening with increasing thermal maturity. Petroleum or related organic fluids are not thought to be the cause of colour change because fluids would cause a pervasive colouration of not only the fossil but the interstitial and surrounding clay matrix. In the fossil record, the colour of the clay matrix is independent of foraminiferal colour.

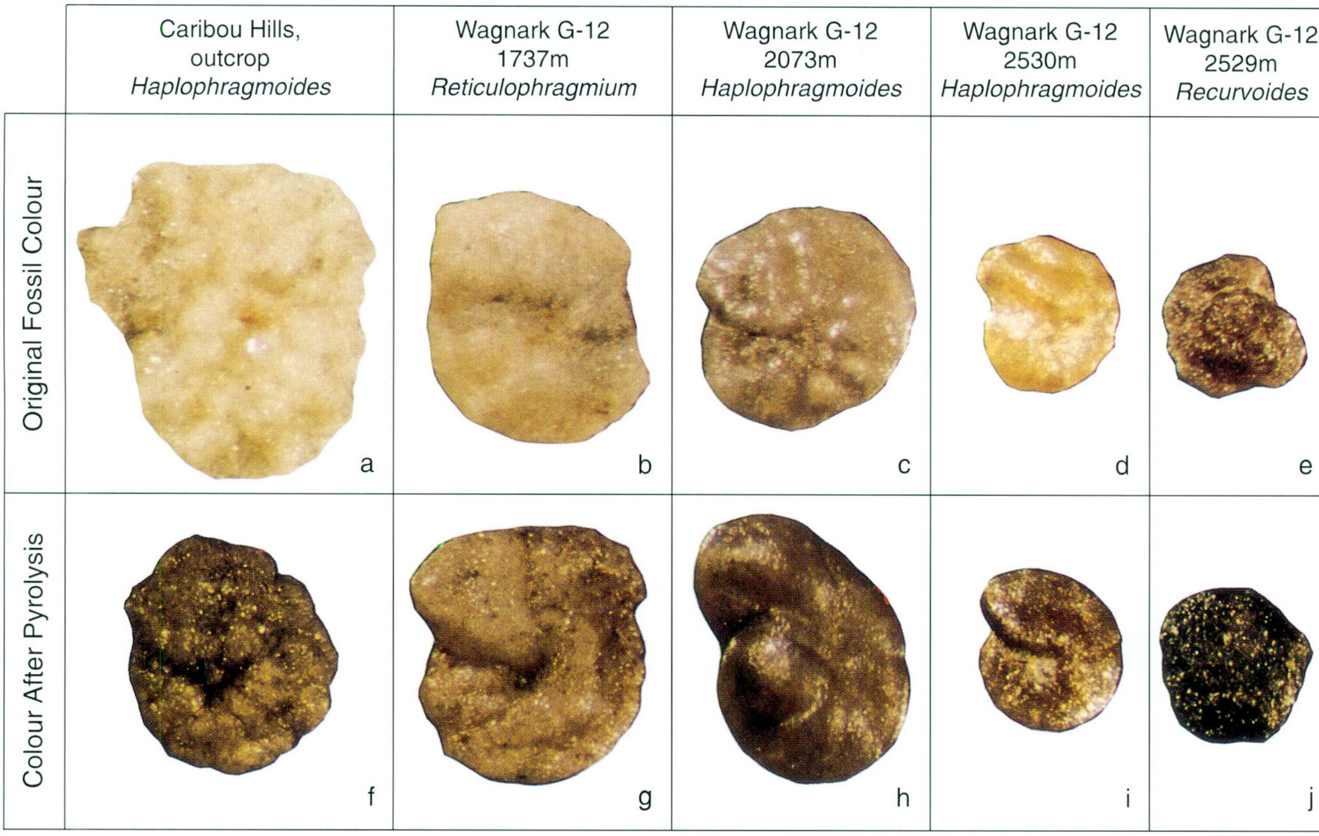

Figure 14. *Examples of fossil colouration before (a to e) and after (f to j) heating by pyrolysis. All specimens are agglutinated foraminifers from strata representing increasing levels of maturation (left to right). Colouration after pyrolysis is consistently darker.* ***Recurvoides*** *(e) contains the greatest amount of organic cement and showed significantly darker colouration after pyrolysis (j).* ***a. Haplophragmoides****, GSC 112268;* ***b. Reticulophragmium****, GSC 112269;* ***c. Haplophragmoides****, GSC 112270;* ***d. Haplophragmoides****, GSC 112271;* ***e. Recurvoides****, GSC 112272;* ***f. Haplophragmoides****, GSC 112273;* ***g. Reticulophragmium****, GSC 112274;* ***h. Haplophragmoides****, GSC 112275;* ***i. Haplophragmoides****, GSC 112276;* ***j. Recurvoides****, GSC 112277.*

BURIAL DIAGENESIS AND MINERALIZATION IN FOSSIL FORAMINIFERS

Independent of colour alteration, there are conspicuous changes in the textural and mineralogical content of the foraminiferal wall as thermal maturity increases. In unaltered Recent agglutinated foraminifers, the wall typically consists of a porous aggregate of detrital quartz grains of various sizes (Figs. 2, 6a). In the fossil record, however, the texture of the agglutinated wall can change drastically and become characterized by a tight, interlocking, crystalline texture (Fig. 6b, c). Silica dominates the geochemistry of these altered microfossils and they are considered "silicified" when they have a glassy translucent appearance, display brittle fracture across grains, and show secondary crystallization of quartz. Silicification of agglutinated foraminifers is well established in sediments that have undergone thermal maturation equivalent to about 0.4 to 0.5%Ro. In addition to quartz, secondary minerals diagnostic of burial diagenesis include kaolin, smectite, illite, chlorite, and carbonate minerals.

Diagenetic effects of burial are not limited to agglutinated tests, but occur also in calcareous-walled foraminifers. Chloritization is the most conspicuous of the mineralogical changes encountered. At thermal maturity levels equivalent to 2%Ro or higher, chloritic clay is precipitated in the chamber cavities of calcareous foraminifers (Fig. 7). Calcium carbonate is also unstable at high temperature/pressure and undergoes recrystallization and possibly replacement by magnesium and/or iron carbonates. At these high levels of thermal maturity, the calcium carbonate of the foraminiferal test can be replaced entirely by chlorite. Chloritized "calcareous" foraminifers have

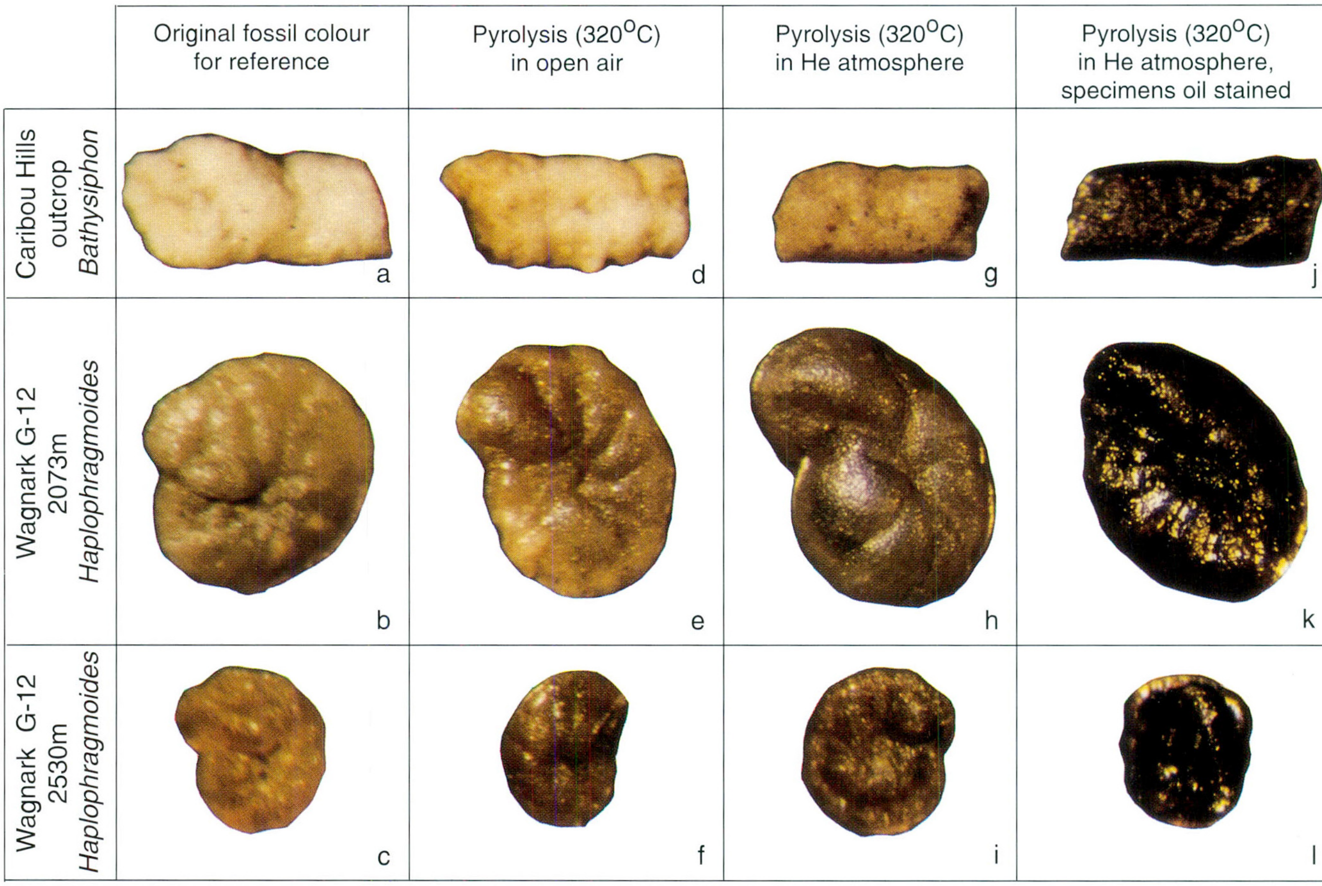

***Figure 15**. Comparison of colouration effects before (a to c) and after pyrolysis heating in the presence of air (d to f), in a helium atmosphere (g to i), and for oil-stained specimens in a helium atmosphere (j to l). **a. Bathysiphon**, GSC 112278; **b. Haplophragmoides**, GSC 112270; **c. Haplophragmoides**, GSC 112271; **d. Bathysiphon**, GSC 112279; **e. Haplophragmoides**, GSC 112280; **f. Haplophragmoides**, GSC 112281; **g. Bathysiphon**, GSC 112282; **h. Haplophragmoides**, GSC 112275; **i. Haplophragmoides**, GSC 112283; **j. Bathysiphon**, GSC 1122847; **k. Haplophragmoides**, GSC 112285; **l. Haplophragmoides**, GSC 112286.*

been observed not only in the Beaufort-Mackenzie area, but also in the Sverdrup Basin of the Arctic Islands and in the Western Canada Sedimentary Basin, indicating that this phenomenon is not an isolated occurrence.

Authigenic mineralization induced through burial diagenesis is progressive with increasing thermal maturity and therefore provides a record for assessing thermal maturity. The zonal scheme presented in Figures 16 and 17 summarizes the textural and mineralogical changes in fossil foraminifers. Four zones (A to D), controlled by pressure/temperature and solution-chemistry-induced changes, are recognized.

The upper part of Zone A (Figs. 16a, 17) represents organically agglutinated foraminifers that have undergone no alteration. Wall texture in foraminifers of Zone A is porous and grains are coated with copious amounts of organic cement. Close examination of agglutinated specimens at high magnification makes it apparent that without the organic cement these specimens would easily disaggregate and never be preserved. No indication of primary mineralization was observed in the Recent agglutinated foraminifers. This excludes specimens of porcelaneous and calcareous agglutinated foraminifers, such as *Sigmoilina* and *Karreriella*. Early diagenetic pyrite mineralization, which reflects bacterial reduction of iron, also is not included in this scheme.

Zone A also includes the initial changes associated with increasing burial depth and temperature. Overburden pressures in this zone are derived from 2 km or slightly more of sediment. Geotemperatures rise to about 75°C and geothermal maturation levels equate to about 0.4%Ro. FCI average values through

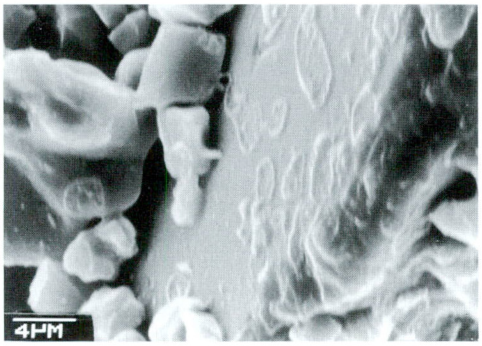

a) *Rhabdammina*,GSC 112288, Recent, North Atlantic.

ZONE A

Burial depth: 0-2400 m

Temperature: 0-75°C

Wall texture unaltered, grains loosely aggregated, some compaction at depth. No secondary mineralization.

FCI: 0-2.5

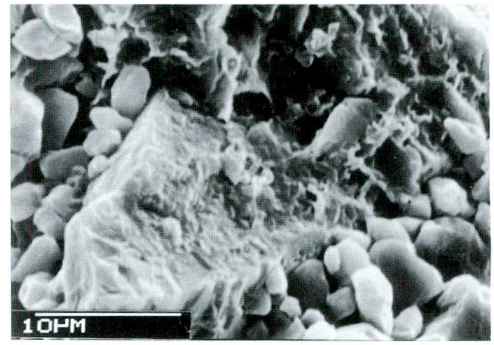

b) *Recurvoides,* GSC 112287, Amauligak J-44, 2260 m.

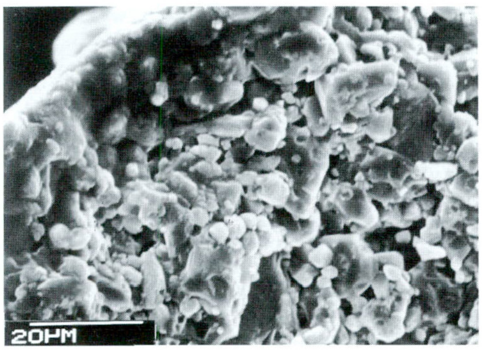

c) *Bathysiphon,* GSC 112288, Amauligak J-44, 2780 m.

ZONE B

Burial depth: 2400-3500 m

Temperature: 75-110°C

Wall texture granular, porosity reduced by quartz mineralization. Organic cement present, slight carbonization and darker colouration.

FCI: 2.5-3.5

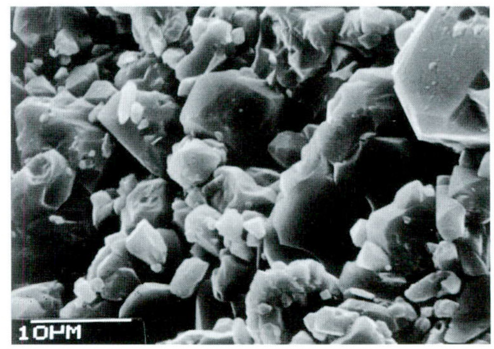

d) *Bathysiphon,* GSC 112288, Amauligak J-44, 2780 m.

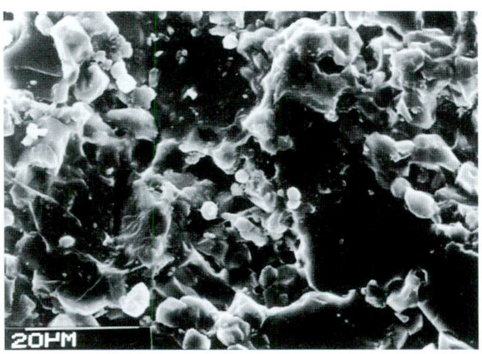

e) *Recurvoides,* GSC 112289, Amauligak J-44, 3599 m.

ZONE C

Burial depth: 3500-5000 m

Temperature: 110-140°C

Wall texture crystalline, porosity reduced by mineralization of quartz, kaolin and smectite precipitated. Organic cement carbonized to dark brown colour.

FCI:~3.5-7.5

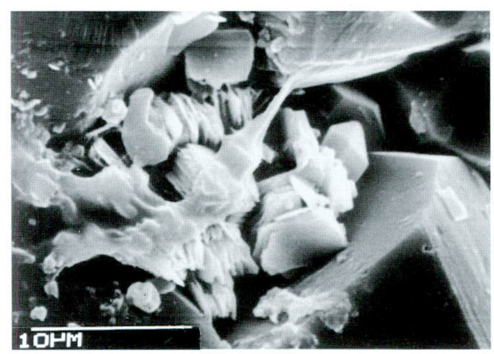

f) *Labrospira,* GSC 112290, Amauligak J-44, 3599 m.

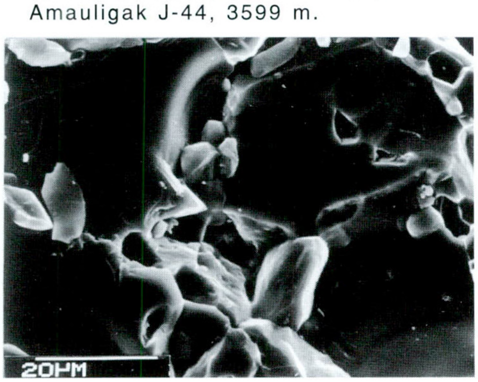

g) *Haplophragmoides,* GSC 112236, Roland Bay L-41, 2208 m.

ZONE D

Burial depth: ~6-8 km

Temperature: 150-250°C

Wall texture crystalline, porosity negligible, silicification complete, calcite recrystalized, illite and chlorite precipitated. Organic cement carbonized (black).

FCI:~7.5-10

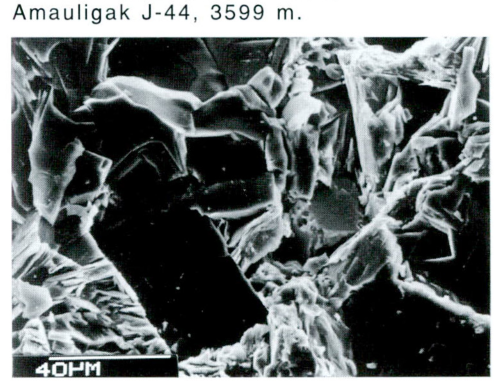

h) *Marginulina,* GSC 112238, Roland Bay L-41, 2164 m.

***Figure 16**. Burial diagenesis in foraminifers. Four zones are recognized from textural and mineralogical changes in the wall of agglutinated and calcareous foraminifers.*

Zone A range from 0 to approximately 2.5. The criteria for recognizing the lower part of Zone A are: 1) a diminution of organic cement, which is not as abundant as in Recent specimens, and 2) a reduction in the porosity of the agglutinated wall due to compression by sediment loading. There are no mineralogic changes recognized in the foraminiferal test at this level of maturation.

Zone B (Figs. 16, 17) is distinguished by the first signs of secondary silica in the form of independent quartz crystals and quartz overgrowths on individual grains in the agglutinated wall. Mineralization at this stage is only partial, hence specimens do not display a crystalline texture. When specimens are fractured or broken, breakage occurs around or between grains rather than across or through grains. Viewed from the exterior, the wall retains its granular porous surface although this factor is variable between species. Internally, organic content is diminished as the glycosaminoglycan cement is gradually carbonized, imparting a pale greyish brown colour to the test. Porosity in the test wall decreases further as quartz overgrowths fill voids, creating a denser, stronger test. Reflectance values in Zone B range from approximately 0.4 to 0.6%Ro and burial depth is in the order of 2.5 to 3.5 km. FCI average values range from approximately 2.5 to 3.5. Paleotemperatures may have ranged from approximately 75 to 110°C.

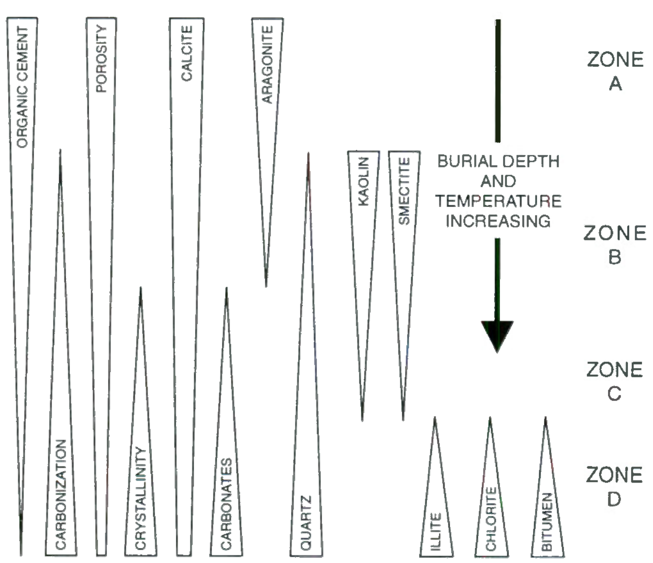

Figure 17. *Generalized trends observed in the organic matter and mineralogy of agglutinated and calcareous foraminifers during burial diagenesis.*

Silicification of the agglutinated wall is well established in Zone C (Figs. 16, 17), which represents thermal maturity levels that exceed approximately 0.6%Ro and FCI average values of approximately 3.5 to 7.5. With silicification, the exterior of the foraminiferal test takes on a glassy lustre, colouration is greyish brown to brownish black, and the test becomes translucent. Examination of the interior of the agglutinated wall reveals a crystalline texture, loss of porosity, and brittle fracture across grain boundaries when the wall is broken. Quartz overgrowths and independent crystals are common to abundant (Fig. 16e, f), but some porosity is still present in the foraminiferal wall and much of the original grain texture can be observed.

Another characteristic of Zone C is the occurrence of clay minerals in minor quantities within the wall of the foraminifer or filling the chamber cavities. Authigenic kaolin booklets and strands of smectitic clay have been documented (Fig. 16f) in the upper part of Zone C (0.6 to 0.7%Ro). These clay minerals have not been observed in foraminifers at higher levels of thermal maturity. This may be modified with future work, since rocks and microfossils from the range of 0.7 to 2.0%Ro have not been examined extensively in this study.

Zone D (Figs. 16, 17) represents the final stage of burial diagenesis recognized in the sections studied from the Beaufort-Mackenzie Basin. The boundary between Zones C and D has not been identified precisely in terms of reflectance but probably lies between 1.0 and 2.0%Ro. Vitrinite reflectance levels associated with Zone D thus range from approximately 2.0 to 4.3%Ro or higher, based on data from the Roland Bay L-41 well, which registered the highest level of thermal maturity in the current study. At these levels of maturity, the foraminiferal test becomes progressively more opaque due to carbonized organic material and FCI average values range from 7.5 to 10. Quartz overgrowths continue to develop and reach their maximum extent, such that most of the original porosity is infilled. The original grain texture of the wall is lost or destroyed by secondary crystallization.

Examination of calcareous foraminifers from the Roland Bay L-41 well, in Zone D at vitrinite reflectance levels of 2.0 to 4.3%Ro, reveals remarkable mineralogical changes beyond the silicification observed in the agglutinated foraminifers. The general exterior morphology of these calcareous foraminifers is intact, but cross-sectional examination of the calcite wall indicates extensive recrystallization and

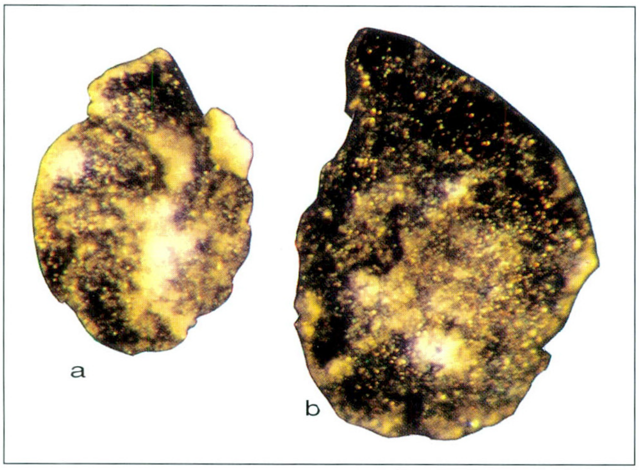

***Figure 18. Lenticulina** coated with black bituminous residue, interior filled by whitish chloritic clay. 18a. GSC 112291 and 18b. GSC 112292 both from Late Jurassic, Kingak Formation, Roland Bay L-41 well, 1586 m.*

mobilization of calcite, and the introduction of significant amounts of secondary chlorite in the interior of the specimen, inter-developed with secondary calcite rhombs (Figs. 7, 16h). Rather than becoming silicified, as in the agglutinated foraminifers, the calcareous foraminifer at high levels of thermal maturity has become recrystallized and chloritized.

Foraminifers from Zone D are also typically coated on the exterior by a brownish black patina which is probably a bituminous residue derived from the condensation of hydrocarbons from Jurassic and Upper Cretaceous shales with relatively high levels of type I organic matter. Chloritized ''calcareous'' specimens, for example, have a discrete outer black coloured layer (Fig. 18) but are white internally.

ORIGIN OF MINERALOGICAL CHANGES

Secondary mineralization in fossil foraminifers is the result of hydrothermal phenomena. Unfortunately, the geochemistry and mineralogy of terrigenous, fine-grained, heterogeneous, rapidly deposited, organic-rich sediments and their associated fluids are among the most complex and difficult geological phenomena to document. Conclusions tend to be empirical rather than directly or analytically determined. Fortunately the end products can be observed and analyzed in great detail using SEM photography and EDX elemental analysis (Fig. 19).

Silicification in foraminifers is the result of quartz overgrowths developed on existing detrital quartz in the foraminiferal wall (Fig. 20). The source of silica for quartz overgrowths is from silica saturated pore-fluids. Silica originally enters the sedimentary system in very low quantities, undersaturated in river and oceanic waters (Krauskopf, 1956; Sayles and Manheim, 1975). Silica then becomes trapped in sediment pore-fluids and begins to evolve with changing geological conditions. Additional SiO_2 may be derived from the destruction of feldspars and the transformation of smectite to illite, as Foscolos and Powell (1980) have postulated for Beaufort-Mackenzie Basin and Sverdrup Basin sediments, but this process is not a necessary prerequisite for silicification. Bloch and Hutcheon (1992) have summarized, from numerous studies of silica concentrations in pore-fluids, that mineral assemblages and temperatures control the amount of pore-fluid silica available, and that with

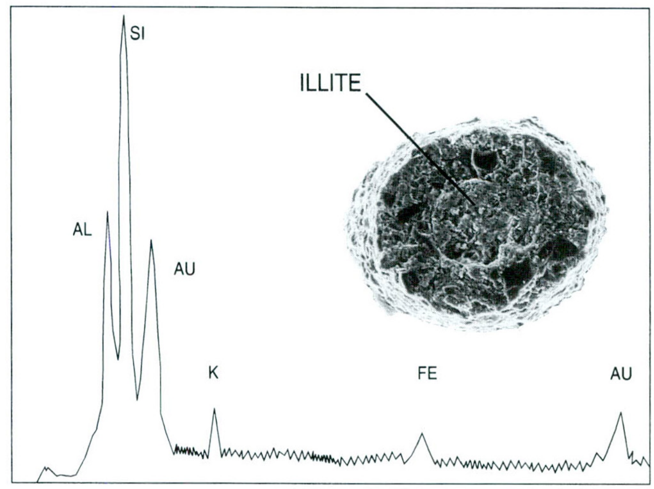

a

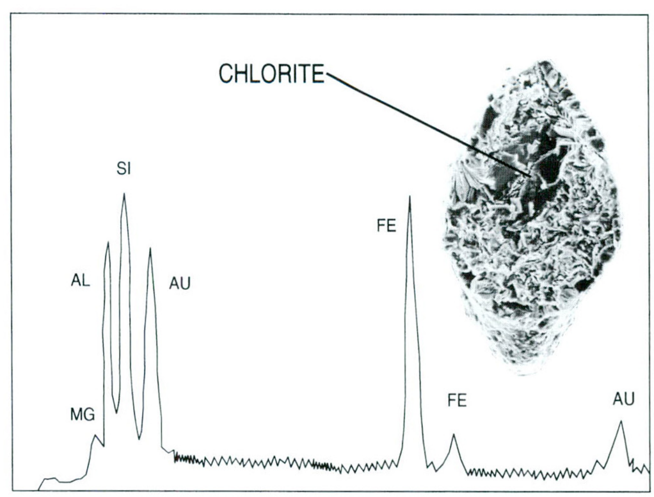

b

***Figure 19.** EDX identification of secondary clay mineralization in fossil foraminifers at relatively high levels of burial diagenesis (Zone D). **a. Bathysiphon** (GSC 112293) infilled with illitic clay, Roland Bay L-41, 670 m; **b. Lenticulina** (GSC 112294) infilled by chloritic clay, Roland Bay L-41, 2438 m.*

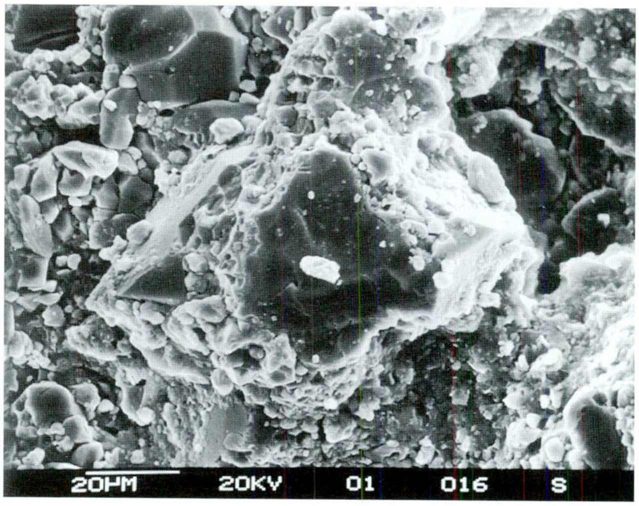

*Figure 20. Pyramidal quartz overgrowths around a primary grain in the wall of an agglutinated foraminifer (**Reticulophragmium**, GSC 112295, Amauligak J-44, 3998 m). Specimen etched slightly in hydrofluoric acid.*

increasing temperature, dissolved SiO_2 concentrations approach saturation.

Authigenic kaolinite, smectite, illite, and chlorite mineralization are well documented in fossil foraminifers from the Beaufort-Mackenzie area (Fig. 16). Low temperature mineralization is characterized by the occurrence of authigenic kaolin booklets in the main chamber cavity of foraminifers and also imbedded in the smaller pore spaces of the agglutinated wall. Smectite also occurs as authigenic strands draped over other mineral grains in the agglutinated wall. The precipitation of kaolin and smectite reflects the content of the early diagenetic and low temperature pore fluids which, in turn, may be influenced by dissolved minerals in groundwaters and by subsurface weathering of minerals. For example, the dissolution of feldspars might lead to the mineralization of kaolin. Chlorite could potentially be precipitated over a broad range of temperature/pressure regimes (Hayes, 1970). As geothermal temperature increases, the solubility of reduced iron also increases, leading to the saturation of ferrous ions in pore-fluids and greater potential for precipitation of chlorite. Empirical evidence indicates that the chlorite occurring in recrystallized calcareous foraminifers in diagenetic Zone D is from a relatively high temperature regime (2 to 4.3%Ro). No chlorite was observed in foraminifers at lower levels of thermal maturity. Chlorite is certainly typical of high thermal maturity assemblages. De Segonzac (1970) summarized that chlorite was characteristic of late catagenetic stages (100 to 200°C) and in a zone (above approximately 200°C) transitional to metamorphic regimes, such as the well known greenschist facies. Foscolos (1992) also recognized a relative increase in chlorite, along with illite, with increased thermal maturation and the disappearance of smectites and kaolinite.

In addition to its role as an indicator of relatively high levels of maturity, chlorite has potential as a geothermometer (Hayes, 1970), based on chlorite polytypism. Such analysis is beyond the scope of this study, but this is a logical area for future attention.

FCI, ZONES OF BURIAL DIAGENESIS, AND THERMAL MATURITY

There are many methods for analyzing thermal maturity. Two of the most common methods, vitrinite reflectance and Rock-Eval pyrolysis (Tmax), have been used in this study to assess the observed progression of changes in fossil foraminifers. Although FCI, VRo, and Tmax methods all generate precise quantifiable values, no rigid correlation of FCI with either VRo or Tmax is attempted due to the inherent difficulties in obtaining unqualifiedly accurate assessments of thermal maturity. General comparisons however can be made.

Vitrinite reflectance is a statistical derivative based on the reflectivity of coaly macerals which increases as thermal maturity progresses. Progressive change is due to the concentration of carbon and loss of hydrogen and oxygen. Vitrinite reflectance is generally the industry standard for measuring thermal maturity and accordingly all of the FCI data derived in the present study are compared to VRo. Rock-Eval pyrolysis, which is based on measuring the products given off by heating fossil organic material to determine thermal maturity, is also used for assessing FCI. VRo and Tmax are subject to variations in original organic type, burial time, reworking, and well cavings. FCI is also subject to most of these variables, but has an advantage in being based on a single group of compounds (glycosaminoglycans) which are biostratigraphically constrained.

Vitrinite reflectance, Tmax, and FCI data are presented in Figures 9, 10, and 11 for the Amauligak J-44, Issungnak 2O-61, and Roland Bay L-41 wells. These data indicate that FCI is most sensitive over a range of VRo values of 0.4 to 0.7%Ro, and Tmax values of 420 to 430°C. At higher levels of thermal maturity (1-2%Ro), FCI changes only slightly from brownish black to black. FCI is therefore an important index of geothermal maturation in the transitional zone between immature (less than 0.3%Ro) and mature (0.5-1.5%Ro) hydrocarbon facies. Moreover, the chemical reactions responsible for the transformation in colour occur fairly rapidly and this is kinetically consistent with the postulated maturation of closely related organic compounds (glycosaminoglycans) which would have a narrow distribution of activation energies.

Estimation of thermal maturity from optical examination of fossils is based on the evaluation of colour as an indicator of maturity. Two main groups of fossils have been used in the past, palynomorphs and conodonts, to determine TAI (Thermal Alteration Index) and CAI (Conodont Alteration Index), respectively. The thermal alteration of Paleozoic–Triassic conodonts cannot be directly compared with foraminifers from the Jurassic–Cenozoic of the Beaufort–Mackenzie Basin. Palynomorph–foraminiferal comparisons are possible, but have not been attempted here because of the complications that could be introduced by the abundance of reworked pollen and spores in rapidly deposited deltaic-dominated sediments of the Beaufort–Mackenzie Basin. This underscores the usefulness of using in situ marine fossils such as foraminifers to determine thermal maturity of marine sedimentary rock. Of course, foraminifers could also be reworked, so care must be taken to assess the reliability of any fossil assemblage.

Diagenetic zones A to D cannot be quantified in the same manner that colouration is in FCI. Changes in the foraminiferal test that have led to the establishment of the zonation are based on numerous presence/absence criteria that could vary depending on the specific geological setting. Zones A to D, however, are thermally controlled and comparison with VRo provides a means to relate these zones to hydrocarbon potential. Zone A corresponds to vitrinite reflectance levels of up to about 0.4%Ro and immature hydrocarbon facies. Zone B, which is recognized chiefly by initial silicification in the agglutinated foraminifer, corresponds to VRo values of approximately 0.4 to 0.5%Ro and is therefore an important index of the transition from immature to mature hydrocarbon facies. Zone C, characterized by the complete silicification of agglutinated foraminifers coupled with the occurrence of diagenetic kaolin and smectite, spans VRo levels of 0.5%Ro to approximately 2.0%Ro, corresponding to mature and overmature (dry gas) facies. Zone D, characterized by thorough silicification, carbonate instability, bitumen coating, and illite and chlorite crystallization, corresponds to VRo levels above approximately 2.0%Ro and hence overmature hydrocarbon facies.

FCI TRENDS IN SIX EXPLORATION WELLS

General trends

Six wells have been chosen to assess foraminiferal colouration in the context of differing geological and geothermal settings in the Beaufort–Mackenzie area. Standard deviations for FCI data are plotted for each well (Fig. 21). Figure 21 illustrates that FCI increases systematically in Arluk E-90, Amauligak J-44, and Amerk O-09 in a nearly linear trend, with increasing depth and temperature. In these wells FCI appears to have good potential as a predictive index of thermal maturation. In the other three wells, however, FCI departs significantly from an ideal progressive linear increase with depth/temperature. In Reindeer D-27 and Roland Bay L-41, FCI increases very little with increasing depth/temperature, and in Wagnark G-12, the FCI trend oscillates in a broad sigmoidal pattern.

Offshore wells

The offshore wells cited above (Arluk E-90, Amauligak J-44, and Amerk O-09) have relatively simple burial histories, and there are no complications introduced by unconformities, structural deformation, or contrasting depositional regimes. Each has a record of essentially continuous terrigenous clastic sedimentation. Reservoir pressures are hydrostatic at Amauligak J-44, whereas overpressure occurs below 2 km and 3 km depth at Arluk E-90 and Amerk O-09, respectively. FCI average values range from 1.06 to 7.0 with FCI generally decreasing northward or basinward into the progressively younger sediments of the basin. Vitrinite reflectance levels in these wells range from 0.30 to 0.60%Ro. Estimated present-day bottom-hole temperatures, based on corrected logging temperatures and drillstem test temperatures, range from a high of 140°C in Arluk E-90 to 105°C in Amerk O-09, and 109°C in Amauligak J-44 (Fig. 22). Temperatures in the Arluk E-90 well are anomalously high with respect to other wells in the area and are not consistent with FCI average values and estimated vitrinite reflectance. Perhaps there has been a recent increase in heat flow at Arluk E-90 and organic matter has had insufficient time to mature, or perhaps the recorded temperatures are incorrect.

Arluk E-90 shows a generalized linear relationship between FCI and increasing burial depth. In detail, however, FCI average values increase downhole in a stepwise manner. There doesn't appear to be any geological or geothermal explanation for this trend and it might be an artifact of drilling procedures since the data is derived from well cuttings.

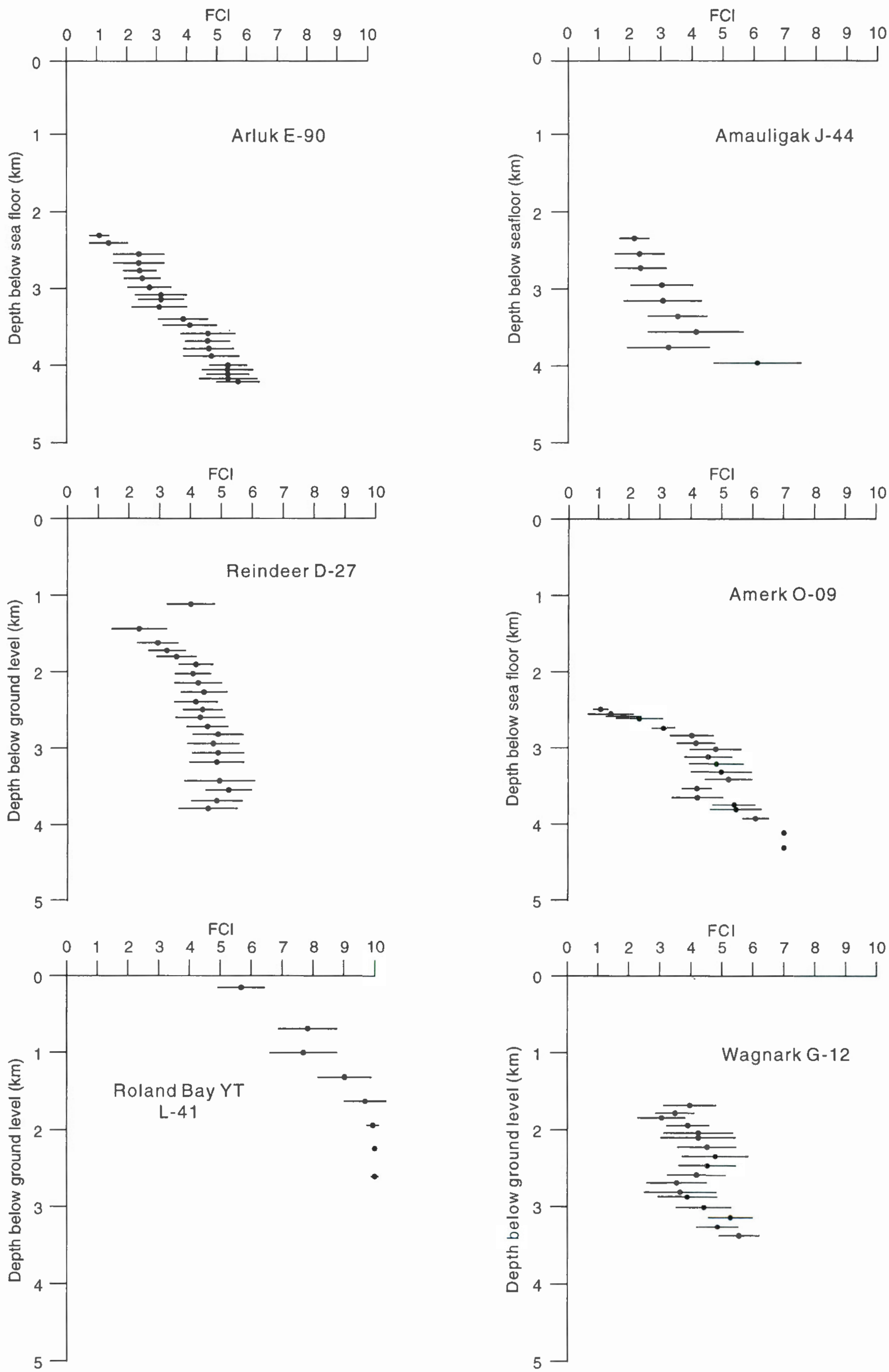

***Figure 21.** Distribution of Foraminiferal Colouration Index (FCI) in six Beaufort–Mackenzie exploration wells. Average FCI and standard deviation from the average value is indicated by the horizontal bars.*

FCI averages in the Amauligak J-44 well increase steadily with depth, and slightly more rapidly in the lower part of the well (Fig. 21). An anomalous FCI value of 3.25 at about 3797 m represents a section barren of in situ fossils but containing caved specimens which result in an erroneously low FCI value. Amauligak J-44 has a calculated present-day temperature of 109°C at 3948 m (Fig. 22) and FCI was measured at 6.29. This contrasts with Arluk E-90, where FCI at a near-equivalent depth is only 5.49 despite an apparently higher present-day heat flow. Thick, rapid deposition of the Pliocene–Pleistocene Iperk Sequence at the Arluk E-90 site might explain the lower maturity levels.

Plots of average FCI in the Amerk O-09 well have a curvilinear trend, with FCI values increasing quickly through the section 2540 to 2870 m, but then at lower rates of increase in the deeper part of the well. The maximum FCI value of 7.00 is also significantly higher in this well than either Arluk E-90 or Amauligak J-44 and probably signifies a longer period of deep burial than the other two wells. Two anomalous FCI values at 3560 and 3680 m are skewed left because of well cavings and are likely barren of in situ foraminifers, judging from the absence of higher FCI values in those two samples. A tapering off of FCI values in the lower part of the well probably indicates that the maturation of foraminiferal organic matter may be slowing down at vitrinite levels of 0.5 to 0.6%Ro.

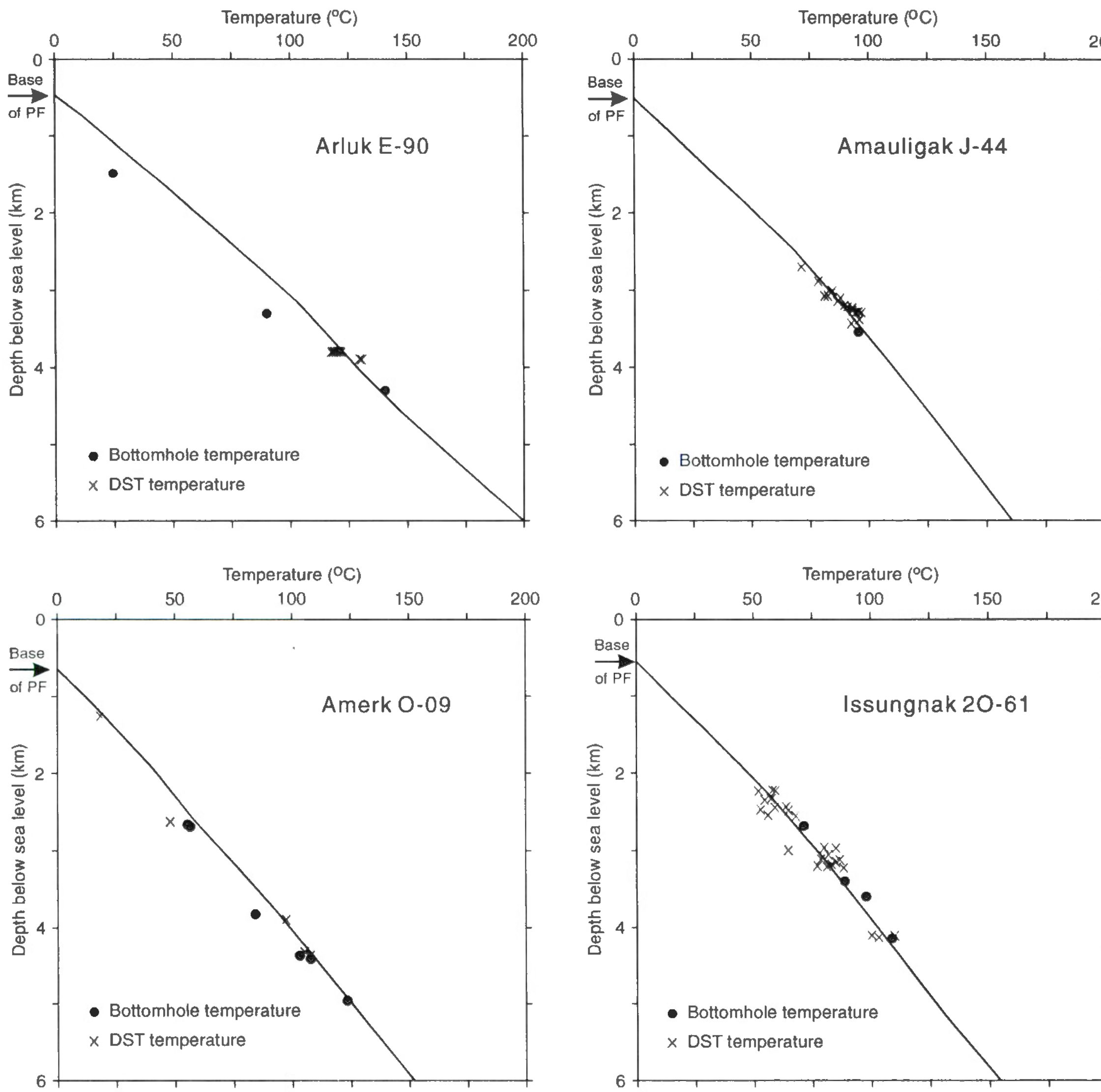

Figure 22. *Temperature versus depth for four offshore Beaufort–Mackenzie exploration wells. Calculated temperatures (solid line) were determined using a modified version of a finite element heat conduction model (Issler and Beaumont, 1988). Corrected bottomhole temperatures and drillstem test temperatures were used to constrain the temperature profiles. The estimated base of permafrost (PF) is assumed to be at 0°C.*

Figure 22 shows temperature-depth profiles for Arluk E-90, Amauligak J-44, Amerk O-09, and Issungnak 2O-61. Temperature profiles were calculated using a modified version of a finite element heat conduction model (Issler and Beaumont, 1988) that includes sediment conductivity variations as a function of lithology, porosity, and temperature. Calculated thermal profiles were constrained by corrected bottomhole temperatures and drillstem test temperatures measured in the study wells. It is unclear whether these temperatures represent maximum burial temperatures, due to uncertainties in reconstructing the history of permafrost development. Permafrost thicknesses typically exceed 500 m in many of the offshore wells of the Beaufort-Mackenzie Basin. Thermal reconstructions for the Amerk O-09 well suggest that temperatures near the base of the well could have been 10°C higher than present values, prior to permafrost development, if permafrost developed gradually throughout the Quaternary period (White and Issler, 1995).

Calculated well temperatures, derived from Figure 22, are plotted with respect to FCI values for the same four wells in Figure 23. The wells are listed in order of decreasing thickness of the Upper Pliocene–Pleistocene Iperk sequence: Arluk E-90 (2036 m); Amauligak J-44 (1570 m); Issungnak 2O-61 (1168 m), and Amerk O-09 (1068 m). Figure 23 shows that FCI values correlate with progressively higher temperature as Pliocene–Pleistocene burial rates increase. This implies there is a heating rate-dependent kinetic effect associated with foraminiferal colour change. If geothermal gradients remained constant and equal to present values during deposition of the Iperk sequence, approximate heating rates are: 24°C/m.y. (Arluk E-90); 15°C/m.y. (Amauligak J-44), and 9°C/m.y. (Issungnak 2O-61, Amerk O-09).

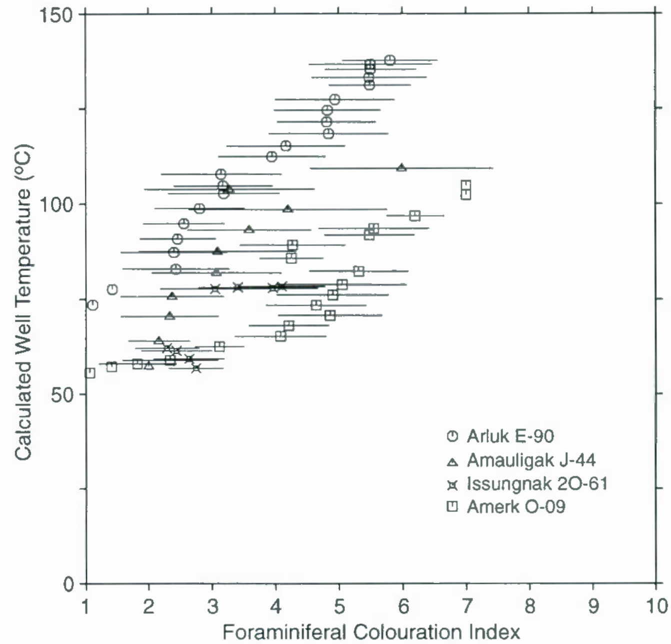

Figure 23. *Present temperature versus FCI for four offshore Beaufort-Mackenzie exploration wells. Calculated well temperatures are from the temperature profiles of Figure 22 for appropriate FCI sample depths. Average FCI values plus one standard deviation (horizontal bars) are shown. Wells are listed in order of decreasing thickness of the Iperk Sequence. FCI values shift to progressively higher temperature with increased burial-related heating rates.*

Onshore wells

The thermal histories of the Reindeer D-27, Roland Bay L-41, and Wagnark G-12 wells (Fig. 21) are longer and geologically more complicated than those discussed above. They are also more difficult to interpret, with the possibility that factors other than geothermal history may come into play. In Reindeer D-27, for example, FCI increases at a steady rate down to about 1908 m, but below that point, FCI increases at a much reduced rate through about 2000 m of section, and then actually decreases in value in samples at 3731 and 3813 m. Examination of the foraminiferal assemblage at those points indicates that the decrease in FCI is valid (i.e., not from well cavings) and occurs in an assemblage dominated by *Bathysiphon* sp. Brownish coloured tests (FCI 5–6) are replaced downsection by greyish, lighter coloured tests (FCI 4–5). Vitrinite reflectance of 0.67%Ro has been measured at 3230 m and the projected vitrinite reflectance at the well's total depth (3861 m) is estimated to be 0.80%Ro. FCI average values near that depth are only 5.08, which is low compared to the associated vitrinite reflectance levels.

No definite explanation of the FCI trends through Reindeer D-27 is proposed here, but an apparent correlation exists between overpressured sections and lower than expected FCI values. In Reindeer D-27, shale porosity measurements (Fig. 24) indicate that overpressuring begins at about 2000 m (Issler, 1992). Furthermore, at 3710 m, coincident with the reversal in FCI values noted above, porosity increases markedly, indicating an even stronger zone of overpressuring at depth. It is possible therefore, that the colour and maturation of foraminiferal organic matter may be affected by the influence of overpressured pore fluids, with the effect of either retarding the reaction or perhaps by leaching colour from the microfossils.

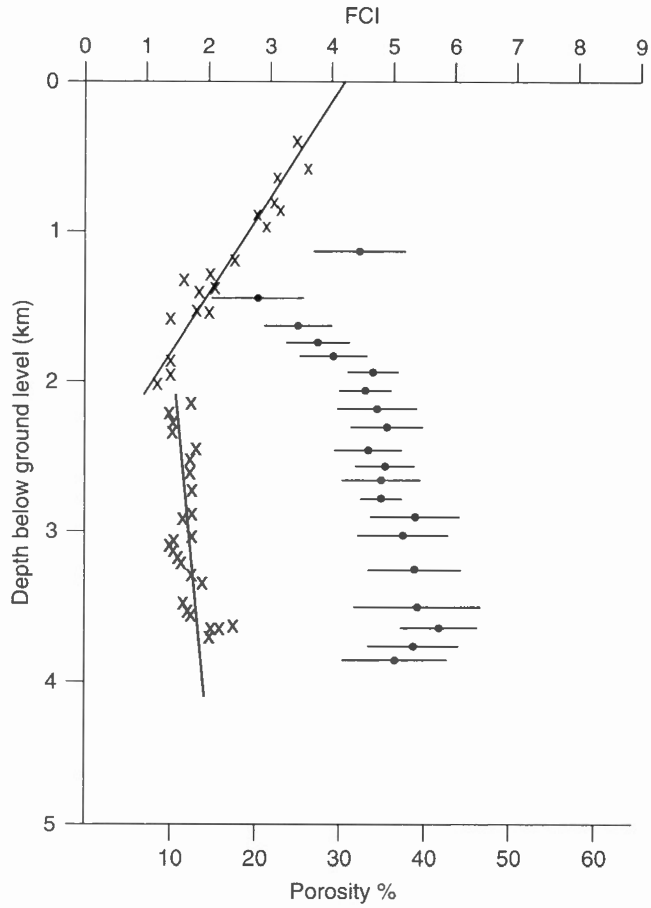

***Figure 24.** Comparison of the distribution of FCI and shale porosity trends in the Reindeer D-27 well, Mackenzie Delta. Porosity estimated from the borehole's sonic log (Issler, 1992). Compaction trends are normal lithostatic down to 2000 m. Increased porosity below that level indicates overpressuring by trapped pore fluids.*

Of the wells considered in this study, Roland Bay L-41 (Figs. 11, 21) has undergone by far the highest level of thermal alteration. Vitrinite reflectance levels of 1.90%Ro near the top of the well to 4.20%Ro at 2245 m (near total well-depth) have been measured. Relatively high maturation levels near the top of the well indicate that several kilometres of section have been eroded from this site. FCI values are high, as expected, through the Roland Bay L-41 well, with averages ranging from 5.73 to 10.0. FCI values increase in a slow, near-linear trend through the first 1500 m in the well, then increase slowly downhole as FCI values reach a maximum of 10.0 at 2195 m. The succession at Roland Bay L-41 does not appear to have been affected by overpressured pore fluids. The observed FCI values may therefore be an accurate reflection of thermal history. As specimens approach pure black in the lower part of the Roland Bay L-41 well, their organic matter has approached total carbonization and they lose their potential for recording further changes in thermal maturity.

Total organic content in the rock matrix in Roland Bay L-41 is as high as 4.94% TOC at 670 m and ranges from 2.0 to 3.0% TOC through much of the well. In core sample 670–678 m, where TOC is at a maximum 4.94, FCI is slightly higher than the general trend. FCI may be influenced slightly by TOC, but apparently not greatly.

The plot of FCI standard deviations for samples from Wagnark G-12 indicate an anomalous but well developed sigmoidal trend with increasing burial depth (Fig. 21). In previous examples from the Amauligak J-44 and Amerk O-09 wells, similar deviations were explained by caved well cuttings, but biostratigraphic considerations rule out this possibility in Wagnark G-12. The well shows two linear trends of increasing FCI offset by a decrease in FCI at about 2300 m. The controlling factor appears to be in the nature, composition, or quantity of the organic cement in different foraminiferal assemblages.

Lithological/depositional differences may also have played a role; the upper section is composed mostly of olive grey shale and the lower section, below about 2350 m, is dominated by uniform, brownish black shale of the lower Mason River and Smoking Hills formations. Rock colours, though different, are more or less consistent through the lower and upper parts of the well and do not parallel FCI trends that appear to be influenced by thermal maturation.

Quantity of organic cement in the foraminiferal wall seems to be the determining factor in the sigmoidal distribution of FCI in the Wagnark G-12 well. Specimens in the upper part of the well are coarser grained and may have greater amounts of cement, although this has not been determined quantitatively. Specimens in the lower half of the well are dominantly very fine grained and perhaps contained lesser amounts or thinner coatings of binding organic cement. Again this has not been quantitatively verified, but there is no doubt that the assemblages are inherently different.

In the Wagnark G-12 well, two genera of foraminifers, *Arenobulimina* (2012–2103 m) and *Recurvoides* (2530–2621 m), were observed to contain conspicuously higher amounts of organic cement than associated foraminifers. The high organic content of these genera influences FCI to some extent, but does not change the overall sigmoidal trend in the well. The peak-abundance of the organic-rich specimens of *Arenobulimina* corresponds to a marked peak in the Rock-Eval Tmax values at 2042 m. The increased

Tmax value probably resulted from a specific change in organic matter type, related directly or indirectly to changes in foraminiferal cement, rather than an abrupt increase in thermal maturity at that level.

CONCLUDING REMARKS

In this paper we have demonstrated conclusively that fossil foraminifers undergo colouration and mineralogical changes with increasing thermal maturity and burial diagenesis. This fact makes them potentially useful tools for understanding the burial history of marine sedimentary rocks. FCI is quick, easy, and inexpensive to apply. In exploration work, for example, quantitative results can be obtained readily at the drillsite using standard micropaleontological techniques. Agglutinated foraminifers are usually abundant in terrigenous clastic rocks, including deltaic deposits, shelf sands, and deep water turbidites, all of which are typical targets for hydrocarbon exploration. Standard geothermal indicators such as vitrinite and palynomorphs are commonly reworked in these sediments. Agglutinated foraminifers are typically in situ in these deposits and therefore might provide a better measure of thermal maturity.

The use of the Munsell Colour Chart in determining FCI provides a reliable standard for accurately assessing colour. Quantitative compilation of individual determinations overcomes the problem of assessing natural variation in fossil populations. Calculation of the average FCI and standard deviation provides a precise numerical value for FCI with a statistical estimation of the probable error.

Histogram distributions of FCI provide an objective method for identifying anomalous (caved or reworked) specimens in well cuttings. Caved specimens are recognized as immature relative to the average FCI. Reworked specimens can be recognized in microfossil assemblages by anomalously high FCI values and anomalous mineralization (eg., silicification and chloritization). Silicified specimens are particularly resistant to weathering and the effects of transportation, so their redeposition can provide potential information on source areas for eroded sediments. In sections that have a substantial erosional unconformity, FCI and burial diagenetic zones may be used to estimate the approximate thickness of eroded sediment.

Since FCI is sensitive to colouration changes at maturation levels that correspond to the early stages of hydrocarbon generation, it can be used for recognizing, mapping, and predicting the upper limits of mature source rocks and zones of high economic potential. The same is true for mineralogic changes such as the silicification of foraminifers. Burial diagenesis zone B (initial silicification of agglutinated foraminifers) approximates the upper level of potential hydrocarbon generation and is therefore an important basinal marker which can easily be recognized and mapped throughout fossiliferous marine sediments.

FCI trends in Beaufort-Mackenzie Basin exploration wells have shown that FCI generally increases in a near linear trend to burial depths of 4 or 5 km, but that significant departures from this trend exist. One notable exception, which coincided with an overpressured zone, showed FCI increasing little over a depth of nearly 2000 m. Thus overpressuring might be a factor in slowing colour change. At relatively high levels of thermal maturation, equivalent to VRo% 2 to 4, FCI was found to change very little (brownish black to black). More dramatic changes in colouration occurred at lower levels of thermal maturity (eg., 0.3 to 0.70%Ro). FCI data from four offshore wells indicate that FCI is sensitive to heating rate, with the most rapidly deposited strata showing the lowest FCI values for a given temperature.

FCI was found to be independent of the colour of associated rocks, but in one well FCI was found to be dependent on changes in the foraminiferal assemblage. Assemblages of different ages had independent FCI trends that increased with depth. Independent trends indicate that FCI cannot be used universally to determine paleotemperatures, but must be calibrated for particular assemblages or depositional episodes. The main purpose of this paper, however, is to establish an objective, quantifiable, and reproducible standard for determining colouration in fossil foraminifers and categorizing the main mineralogical changes that foraminifers undergo through burial diagenesis. Further research needs to be done on the nature of the organic material in foraminifers, the relation between FCI and other maturation indices, such as vitrinite reflectance and the thermal alteration index for palynomorphs. More exhaustive work on the experimental maturation of foraminifers through pyrolysis needs to be done to compare experimental and fossil colouration. A better understanding of diagenetic zones A to D could be obtained from additional data collection and more detailed research on the diagenetic history of foraminifers, silica, and clay minerals, in particular. The Beaufort-Mackenzie Basin has an abundance of data from rocks that are immature to marginally mature. FCI and burial diagenesis zones need to be assessed in other geological basins and at higher levels of thermal maturation in future research.

REFERENCES

Ainsworth, N.R. Burnett, R.D., and Kontrovitz, M.
1990: Ostracod colour change by thermal alteration, offshore Ireland and Western UK. Marine and Petroleum Geology, v. 7, p. 288-297.

Alabusheva, A.V.
1990: A relationship between the colour of foraminifer tests and the grade of catagenesis of organic matter in clastic rocks. International Geology Review, v. 32, p. 1166-1169.

Bender, H.
1989: Gehauseaufbau, Gehausegenese und Biologie agglutinierter Foraminiferen (Sarcodina, Textulariina). Jahrbuch der Geologischen Bundesanstalt, v. 132, p. 259-347.

Bender, H. and Hemleben, Ch.
1988: Constructional aspects in test formation of some agglutinated foraminifera. Abhandlungen der Geologischen Bundesanstalt, v. 41, p. 13-21.

Bloch, J. and Hutcheon, I.
1992: Shale diagenesis: a case study from the Albian Harmon Member, Western Canada. Clays and Clay Minerals, v. 40, p. 682-699.

Chilingarian, G.V. and Wolf, K.H.
1988: Diagenesis, II. Developments in Sedimentology, v. 43, 268 p.

De Segonzac, G.D.
1970: The transformation of clay minerals during diagenesis and low-grade metamorphism: a review. Sedimentology, v. 15, p. 281-346.

Epstein, A.G., Epstein, J.B., and Harris, L.D.
1977: Conodont colour alteration - an index to organic metamorphism. United States Geological Survey, Professional Paper 995, 27 p.

Foscolos, A.E.
1992: Catagenesis of argillaceous sedimentary rocks. *In* Diagenesis, I.A. McIlreath and D.W. Morrow (eds.). Geoscience Canada, Reprint Series 4, p. 177-187.

Foscolos, A.E. and Powell, T.G.
1980: Mineralogical and geochemical transformation of clays during catagenesis and their relation to oil generation. *In* Facts and Principles of World Petroleum Occurrence, A.D. Miall (ed.). Canadian Society of Petroleum Geologists, Calgary, p. 153-172.

Goodarzi, F.
1985: Reflected light microscopy of chitinozoan fragments. Marine and Petroleum Geology, v. 2, p. 72-78.

Goodarzi, F. and Higgins, A.C
1987: Optical properties of scolecodonts and their use as indicators of thermal maturity. Marine and Petroleum Geology, v. 4, p. 353-359.

Goodarzi, F. and Norford, B.S.
1989: Variation of graptolite reflectance with depth of burial. International Journal of Coal Geology, v. 11, p. 127-141.

Hayes, J.B.
1970: Polytypism of chlorite in sedimentary rocks. Clays and Clay Minerals, v. 18, p. 285-306.

Hedley, R.H.
1963: Cement and iron in the arenaceous foraminifera. Micropaleontology, v. 9, p. 433-441.

Hemleben, Ch., Spindler, M., and Anderson, O.R.
1988: Modern Planktonic Foraminifera. Springer-Verlag, New York, 363 p.

Hitchon, B., Underschultz, J.R., Bachu, S., and Sauverplane, C.M.
1990: Hydrogeology, geopressures and hydrocarbon occurrences, Beaufort-Mackenzie Basin. Bulletin of Canadian Petroleum Geology, v. 38, p. 215-235.

Issler, D.R.
1992: A new approach to shale compaction and stratigraphic restoration, Beaufort-Mackenzie Basin and Mackenzie corridor, northern Canada. American Association of Petroleum Geologists Bulletin, v. 76, p. 1170-1189.

Issler, D.R. and Beaumont, C.
1988: A finite element model of the subsidence and thermal evolution of extensional basins: application to the Labrador continental margin. *In* Thermal History of Sedimentary Basins - Methods and Case Histories, N.D. Naeser and T.H. McCulloh (eds.), Springer-Verlag, New York, p. 239-267.

Issler, D.R. and Snowdon, L.R.
1990: Hydrocarbon generation kinetics and thermal modelling, Beaufort-Mackenzie Basin. Bulletin of Canadian Petroleum Geology, v. 38, p. 1-16.

Krauskopf, K.B.
1956: Dissolution and precipitation of silica at low temperatures. Geochimica et Cosmochimica Acta, v. 10, p. 1-26.

Langer, M.R.
1992: Biosynthesis of glycosaminoglycans in foraminifera: a review. Marine Micropaleontology, v. 19, p. 245-255.

Majorowicz, J.A. and Dietrich, J.R.
1989: Comparison of the geothermal and organic maturation gradients of the central and southwestern Beaufort-Mackenzie Basin, Yukon and Northwest Territories. *In* Current Research, Part G, Geological Survey of Canada, Paper 89-1G, p. 63-67.

McNeil, D.H., Goodarzi, F., Snowdon, L.R., and Foscolos, A.E.
1989: Colouration and silicification - Agglutinated foraminifers as indicators of organic maturity level and burial diagenesis. NATO Advanced Study Institutes Programme, International Workshop on Agglutinated Foraminifers, Programme and Abstracts, p. 28.

McNeil, D.H., Goodarzi, F., Snowdon, L.R., and Foscolos, A.E.
1990: Agglutinated foraminifers as indices of thermal maturity. Fourth International Symposium on Benthic Foraminifera, Sendai, Japan, Program and Abstracts, p. 40, 41.

Munsell Colour
1975 edition: Munsell Soil Colour Charts. Macbeth Division of Kollmorgen Corporation, Baltimore, Maryland.

Rejebian, V.A., Harris, A.G., and Huebner, J.S.
1987: Conodont colour and textural alteration: an index to regional metamorphism, contact metamorphism, and hydrothermal alteration. Geological Society of America Bulletin, v. 99, p. 471–479.

Reiser, H.
1988: Aragonit/Calcit-Transformation bei Foraminiferengehausen – Möglichkeit zur Rekonstruktion von Paläotemperaturen des Untergrundes. Erdol Erdgas Kohle, Geologie, no. 5, 4 p.

Robert, P.
1985: Organic Metamorphism and Geothermal History. Microscopic Study of Organic Matter and Thermal Evolution of Sedimentary Basins. Elf-Aquitaine and D. Reidel Publishing Co., the Netherlands, 311 p.

Rosen, R.N.
1991: Significance of discoloration in arenaceous Foraminifera. Transactions – Gulf Coast Association of Geological Societies, v. 41, p. 564–569.

Sayles, F.L. and Manheim, F.T.
1975: Interstitial solutions and diagenesis in deeply buried marine sediments: results from the Deep Sea Drilling Project. Geochimica et Cosmochimica Acta, v. 39, p. 103–127.

Sidner, B.R. and McKee, T.R.
1975: Diagenesis of microfaunal remains from the Gyre Basin. *In* Submarine geomorphology and sedimentation patterns of the Gyre intraslope basin, northwest Gulf of Mexico, A.H. Bouma, L.B. Smith, B.R. Sidner, T.R. McKee, (eds.). Texas A & M University, Department of Oceanography, Technical Report No. 75-9-T, Appendix B, p. 132–140.

1976: Geochemical controls on vertical distribution of iron-rich agglutinated foraminifers in late Quaternary continental slope sediments from northwest Gulf of Mexico. American Association of Petroleum Geologists Bulletin, v. 60, p. 722–723.

Staplin, F.L.
1969: Sedimentary organic matter, organic metamorphism, and oil and gas occurrence. Bulletin of Canadian Petroleum Geology, v. 17, p. 47–66.

Weiner, S. and Erez, J.
1984: Organic matrix of the shell of the foraminifer, *Heterostegina depressa*. Journal of Foraminiferal Research, v. 14, p. 206–212.

White, J.M. and Issler, D.R.
1995: Neogene and Quaternary climate and biostratigraphy: why should the oil and gas industry care? *In* Proceedings of the Oil and Gas Forum '95 – Energy from Sediments, J.S. Bell, T.D. Bird, T.L. Hillier, and P.L. Greener (eds.). Geological Survey of Canada, Open File 3058, p. 501–508.

APPENDIX 1

Foraminiferal colouration index (FCI) data for seven exploration wells in the Beaufort–Mackenzie Basin are provided in this appendix. All data are from composited well cuttings, with the exception of core data from Issungnak 2O-61. Sampled units are indicated in metres or feet below kelly bushing (KB) and the true vertical depth (TVD) for the mid-point of the sampled section is indicated in metres below either ground level (GL) or sea level (SL).

FCI data and averages from Amerk O-09 (well cuttings)

Depth (m below KB)	Average TVD (m below SL)	FCI data										Average FCI
		1	2	3	4	5	6	7	8	9	10	
2540–2570	2513	17	1									1.06 ± 0.24
2600–2630	2573	53	26	1			1					1.41 ± 0.77
2630–2660	2603	22	49	6	1							1.82 ± 0.62
2660–2690	2633	11	21	33								2.34 ± 0.76
2780–2810	2753		3	145	22	1						3.12 ± 0.39
2870–2900	2843			21	58	26	2					4.08 ± 0.72
2960–2990	2933			3	16	9						4.21 ± 0.63
3050–3080	3023			6	18	46	18					4.86 ± 0.82
3140–3170	3113	2		12	59	118	17					4.64 ± 0.79
3230–3260	3203			2	7	13	8					4.90 ± 0.88
3320–3350	3293	1			8	18	12	1				5.05 ± 1.01
3440–3470	3413			1	6	18	23					5.31 ± 0.78
3560–3590	3533				3	1						4.25 ± 0.50
3680–3710	3653			5	10	10	1					4.27 ± 0.83
3770–3800	3743				8	18	39					5.48 ± 0.71
3830–3860	3803			2	2	5	24					5.55 ± 0.87
3950–3980	3923						4	1				6.20 ± 0.45
4160–4190	4133							3				7
4250–4280	4223			1				2				7

FCI data and averages from Arluk E-90 (well cuttings)

Depth (m below KB)	Average TVD (m below SL)	FCI data										Average FCI
		1	2	3	4	5	6	7	8	9	10	
2360–2364	2291	16	2									1.11 ± 0.32
2456–2486	2400	80	33	9								1.42 ± 0.63
2603–2621	2541	10	46	36	4	3						2.43 ± 0.85
2720–2735	2657	34	99	86	23							2.40 ± 0.85
2816–2831	2753	6	180	141	7		1					2.46 ± 0.60
2921–2939	2859	8	149	161	15	1						2.56 ± 0.64
3032–3044	2967	6	81	162	33	2	1					2.81 ± 0.71
3134–3152	3072	4	55	96	90	11						3.19 ± 0.88
3200–3215	3137	3	32	101	67	3	1					3.18 ± 0.78
3305–3320	3242	2	6	19	10	3						3.15 ± 0.95
3455–3470	3392		10	55	124	48	7					3.95 ± 0.84
3548–3563	3485		1	87	120	97	17	4				4.17 ± 0.93
3653–3668	3590		1	22	66	126	54	8				4.84 ± 0.94
3758–3773	3695			6	83	104	50					4.81 ± 0.78
3863–3878	3800			13	72	105	53	1				4.82 ± 0.84
3956–3974	3894			14	95	109	82	11				4.94 ± 0.94
4082–4097	4019				3	26	28	2				5.49 ± 0.65
4145–4160	4082				5	8	13	3				5.48 ± 0.91
4196–4232	4143				2	9	12	1				5.5 ± 0.72
4250–4265	4187				2	7	4	3				5.5 ± 0.97
4286–4290	4217				1	3	10	2				5.81 ± 0.75

FCI data and averages from Amauligak J-44 (well cuttings)

Depth (m below KB)	Average TVD (m below SL)	FCI data 1	2	3	4	5	6	7	8	9	10	Average FCI
2200–2210	2150		1									2
2395–2405	2345	8	130	34	1							2.16 ± 0.49
2597–2603	2547	23	42	62	2							2.33 ± 0.78
2780–2804	2730	34	56	90	6							2.37 ± 0.82
2999–3005	2949	8	3	22	23							3.07 ± 1.02
3197–3203	3147	5	2	17	7	1	2					3.09 ± 1.24
3398–3404	3348	3	25	133	101	42	11					3.59 ± 0.97
3599–3605	3549	9	6	4	16	31	14					4.20 ± 1.56
3797–3803	3747	14	19	22	23	14	8					3.28 ± 1.34
3998–4002	2948		5	9	5	18	52	44	15			5.99 ± 1.44

FCI data and averages from Issungnak 2O-61 (core samples)

Depth (m below KB)	Average TVD (m below SL)	FCI data 1	2	3	4	5	6	7	8	9	10	Average FCI
2403.9–2406.9	2238		5	15								2.75 ± 0.44
2508–2511	2328		22	31	2							2.64 ± 0.56
2594.3–2597.3	2402	1	37	29	1							2.44 ± 0.56
2621.2–2624.2	2425		30	10	1							2.29 ± 0.51
3272–3275	2978		23	32	19	4						3.05 ± 0.87
3281–3283	2986			32	59	27						3.96 ± 0.71
3288–3291	2992		1	37	20	3						3.41 ± 0.62
3297–3300	3000			16	57	22	2					4.10 ± 0.68

FCI data and averages from Wagnark G-12 (well cuttings)

Depth (ft. below KB)	Average TVD (m below GL)	FCI data 1	2	3	4	5	6	7	8	9	10	Average FCI
5500–5600	1692			2	2	2						4.0 ± 0.89
5800–5900	1783			35	18	6						3.51 ± 0.68
6000–6100	1844		15	40	10	5						3.07 ± 0.80
6300–6400	1936		6	13	63	20						3.95 ± 0.75
6700–6800	2057		8	47	63	48	23	7				4.27 ± 1.17
6900–7000	2118		12	60	80	58	41	6	2			4.32 ± 1.23
7300–7400	2240		1	15	31	41	19					4.58 ± 0.97
7700–7800	2362		1	14	36	37	40	4				4.86 ± 1.09
8100–8200	2484		1	2	36	24	11		1			4.61 ± 0.91
8500–8600	2606		1	31	39	42	11					4.25 ± 0.96
8800–8900	2698		6	15	16	6	1					3.57 ± 0.97
9200–9300	2819		10	13	11	14	1					3.65 ± 1.16
9400–9500	2880		1	5	8	4	1					3.95 ± 0.97
9900–10000	3033			3	7	8	2					4.45 ± 0.89
10300–10400	3155			1	11	40	43	2				5.35 ± 0.75
10700–10800	3277				27	51	19					4.92 ± 0.69
11100–11200	3399			1	5	16	52	1				5.63 ± 0.69

FCI data and averages from Reindeer D-27 (well cuttings)

Depth (ft. below KB)	Average TVD (m below GL)	FCI data										Average FCI
		1	2	3	4	5	6	7	8	9	10	
3697–3705	1123		2	36	72	144	19					4.52±0.84
4763–4790	1451		42	33	10	6						2.78±0.89
5322–5345	1621		6	58	35	7						3.41±0.70
5650–5690	1723		35	43	10							3.72±0.66
5900–5990	1807		1	15	51	18	1					4.03±0.69
6260–6350	1917			5	56	122	3					4.66±0.56
6660–6750	2039			3	103	126	7	1				4.58±0.59
7040–7190	2164			4	50	53	26					4.76±0.80
7440–7590	2286			1	49	72	38					4.92±0.75
7960–8070	2438				52	46	16					4.68±0.71
8360–8390	2548			3	50	141	34	1				4.91±0.66
8640–8790	2651			8	62	89	44					4.83±0.81
9080–9150	2773			10	42	246	73	1		1		5.05±0.68
9440–9510	2883			1	46	123	139	14	4	1		5.41±0.86
9800–9950	3005			5	44	90	93	7				5.22±0.85
10200–10320	3122			6	49	91	67	2	1	3		5.11±0.96
10560–10670	3231				20	47	42	11	1			5.39±0.90
11416–11425	3476		2	27	33	49	141	42				5.45±1.18
11720–11950	3602			3	9	55	127	30	1			5.78±0.77
12240–12310	3737			2	25	29	72	2				5.36±0.86
12510–12660	3831			9	18	52	40	1		1		5.08±0.97

FCI data and averages from Roland Bay L-41 (well cuttings)

Depth (ft. below KB)	Average TVD (m below GL)	FCI data										Average FCI
		1	2	3	4	5	6	7	8	9	10	
400–600	145				3	13	23	5	1			5.73±0.83
2200–2300	674					1	7	36	27	10	6	7.78±1.14
3200–3300	983					4	44	74	59	35	23	7.61±1.26
4200–4300	1288						3	9	30	36	57	9.00±1.06
5200–5300	1593							3	3	7	44	9.61±0.82
6200–6300	1898									5	108	9.96±0.21
7200–7300	2202										100	10
8400–8500	2568									2	113	9.98±0.13

APPENDIX 2

List of illustrated type specimens and locality information. All specimens are stored in the National Type Collection in Ottawa, but may be stored temporarily at GSC Calgary.

Figure 1. *Rhabdammina*, GSC 112227, Holocene, Baltimore Canyon, North Atlantic Ocean

Figure 2. *Rhabdammina,* GSC 112228, Holocene, Baltimore Canyon, North Atlantic Ocean

Figures 5 and 9.
(9a) *Haplophragmoides*, GSC 112229, Amauligak J-44, 2648 m, Oligocene, Kugmallit Sequence
(9b) *Haplophragmoides*, GSC 112230, Amauligak J-44, 2900 m, Oligocene, Kugmallit Sequence
(9c) *Labrospira*, GSC 112231, Amauligak J-44, 3887 m, Oligocene, Kugmallit Sequence
(9d) *Labrospira*, GSC 112232, Amauligak J-44, 3950 m, Oligocene, Kugmallit Sequence
(9e) *Labrospira*, GSC 112233, Amauligak J-44, 3998 m, Oligocene, Kugmallit Sequence

Figure 6a. *Recurvoides*, GSC 112234, Holocene, Baltimore Canyon, North Atlantic Ocean

Figure 6b. *Reticulophragmium*, GSC 112235, Ukalerk 2C-50, 4121 m, Oligocene

Figure 6c. *Haplophragmoides,* GSC 112236, Roland Bay L-41, 2208 m, Jurassic, Kingak Formation

Figure 7a. Nodosarid, GSC 112237, Oligocene, Biarritz, France

Figure 7b, c, d. *Marginulina,* GSC 112238, Roland Bay L-41, 2165 m, Late Jurassic, Kingak Formation

Figure 8(0). *Recurvoides*, GSC 112239, Holocene, Baltimore Canyon, North Atlantic Ocean

Figure 8(1). *Bathysiphon,* GSC 112240, Amauligak J-44, 2260 m, Late Oligocene, Mackenzie Bay Sequence

Figure 8(2). *Haplophragmoides*, GSC 112241, Amauligak J-44, 2648 m, Oligocene, Kugmallit Sequence

Figure 8(3). *Haplophragmoides*, GSC 112242, Amauligak J-44, 2648 m, Oligocene, Kugmallit Sequence

Figure 8(4). *Reticulophragmium*, GSC 112243, Amauligak J-44, 2900 m, Oligocene, Kugmallit Sequence

Figure 8(5). *Labrospira*, GSC 112244, Amauligak J-44, 3220 m, Oligocene, Kugmallit Sequence

Figure 8(6). *Labrospira,* GSC 112245, Amauligak J-44, 3656 m, Oligocene, Kugmallit Sequence

Figure 8(7). *Labrospira*, GSC 112246, Amauligak J-44, 3887 m, Oligocene, Kugmallit Sequence

Figure 8(8). *Haplophragmoides*, GSC 112247, Amauligak J-44, 3998 m, Oligocene, Kugmallit Sequence

Figure 8(9). *Haplophragmoides,* GSC 112248, Roland Bay L-41, 1280 m, Early Cretaceous, Mount Goodenough Formation

Figure 8(10). *Haplophragmoides*, GSC 112249, Roland Bay L-41, 1891 m, Jurassic, Kingak Formation

Figure 10a. *Haplophragmoides,* GSC 112250, Issungnak 2O-61, 2508 m, Oligocene, Kugmallit Sequence

Figure 10b. *Labrospira*, GSC 112251, Issungnak 2O-61, 3297 m, Oligocene, Kugmallit Sequence

Figure 11a. *Haplophragmoides*, GSC 112252, Roland Bay L-41, 122 m, Maastrichtian, Tent Island Formation

Figure 11b. *Bathysiphon*, GSC 112253, Roland Bay L-41, 670 m, Turonian, Boundary Creek Formation

Figure 11c. *Haplophragmoides*, GSC 112254, Roland Bay L-41, 1280 m, Early Cretaceous, Mount Goodenough Formation

Figure 11d. *Haplophragmoides*, GSC 112255, Roland Bay L-41, 1585 m, Jurassic, Kingak Formation

Figure 12a. *Rhabdammina*, GSC 112256, Holocene, Baltimore Canyon, North Atlantic Ocean

Figure 12b. *Recurvoides*, GSC 112257, Holocene, Baltimore Canyon, North Atlantic Ocean

Figure 12c. *Karreriella*, GSC 112258, Holocene, Baltimore Canyon, North Atlantic Ocean

Figure 12d. *Globorotalia*, GSC 112259, Holocene, Baltimore Canyon, North Atlantic Ocean

Figure 12e. *Cibicidoides*, GSC 112260, Natiak O-44, 880 m, Pliocene, Iperk Sequence

Figure 12f. Ostracod, GSC 112261, Holocene, Baltimore Canyon, North Atlantic Ocean

Figure 13a. *Rhabdammina*, GSC 112262, Holocene, Baltimore Canyon, North Atlantic Ocean

Figure 13b. *Recurvoides*, GSC 112263, Holocene, Baltimore Canyon, North Atlantic Ocean

Figure 13c. *Karreriella*, GSC 112264, Holocene, Baltimore Canyon, North Atlantic Ocean

Figure 13d. *Globorotalia*, GSC 112265, Holocene, Baltimore Canyon, North Atlantic Ocean

Figure 13e. *Cibicidoides*, GSC 112266, Natiak O-44, 880 m, Pliocene, Iperk Sequence

Figure 13f. Ostracod, GSC 112267, Holocene, Baltimore Canyon, North Atlantic Ocean

Figure 14a. *Haplophragmoides*, GSC 112268, GSC Locality C-79716, Douglas Creek, Northwest Territories (NWT), Maastrichtian, Mason River Formation

Figure 14b. *Reticulophragmium*, GSC 112269, Wagnark G-12, 1737 m, Paleocene, Ministicoog Member, Moose Channel Formation

Figure 14c. *Haplophragmoides*, GSC 112270, Wagnark G-12, 2073 m, Maastrichtian, Mason River Formation

Figure 14d. *Haplophragmoides*, GSC 112271, Wagnark G-12, 2530 m, Maastrichtian, Mason River Formation

Figure 14e. *Recurvoides*, GSC 112272, Wagnark G-12, 2530 m, Maastrichtian, Mason River Formation

Figure 14f. *Haplophragmoides*, GSC 112273, GSC Locality C-79716, Douglas Creek, Northwest Territories (NWT), Maastrichtian, Mason River Formation

Figure 14g. *Reticulophragmium*, GSC 112274, Wagnark G-12, 1737 m, Paleocene, Ministicoog Member, Moose Channel Formation

Figure 14h. *Haplophragmoides*, GSC 112275, Wagnark G-12, 2073 m, Maastrichtian, Mason River Formation

Figure 14i. *Haplophragmoides*, GSC 112276, Wagnark G-12, 2530 m, Maastrichtian, Mason River Formation

Figure 14j. *Recurvoides*, GSC 112277, Wagnark G-12, 2530 m, Maastrichtian, Mason River Formation

Figure 15a. *Bathysiphon*, GSC 112278, GSC Locality C-79716, Douglas Creek, Northwest Territories (NWT), Maastrichtian, Mason River Formation

Figure 15b. *Haplophragmoides*, [GSC 112270, see Fig. 14c]

Figure 15c. *Haplophragmoides*, [GSC 112271, see Fig. 14d]

Figure 15d. *Bathysiphon*, GSC 112279, GSC Locality C-79716, Douglas Creek, Northwest Territories (NWT), Maastrichtian, Mason River Formation

Figure 15e. *Haplophragmoides*, GSC 112280, Wagnark G-12, 2073 m, Maastrichtian, Mason River Formation

Figure 15f. *Haplophragmoides*, GSC 112281, Wagnark G-12, 2530 m, Maastrichtian, Mason River Formation

Figure 15g. *Bathysiphon*, GSC 112282, GSC Locality C-79716, Douglas Creek, Northwest Territories (NWT), Maastrichtian, Mason River Formation

Figure 15h. *Haplophragmoides*, [GSC 112275, see Fig. 14h]

Figure 15i. *Haplophragmoides*, GSC 112283, Wagnark G-12, 2530 m, Maastrichtian, Mason River Formation

Figure 15j. *Bathysiphon*, GSC 112284, GSC Locality C-79716, Douglas Creek, Northwest Territories (NWT), Maastrichtian, Mason River Formation

Figure 15k. *Haplophragmoides*, GSC 112285, Wagnark G-12, 2073 m, Maastrichtian, Mason River Formation

Figure 15l. *Haplophragmoides*, GSC 112286, Wagnark G-12, 2530 m, Maastrichtian, Mason River Formation

Figure 16a. *Rhabdammina*, [GSC 112228, see Fig. 2]

Figure 16b. *Recurvoides*, GSC 112287, Amauligak J-44, 2260 m, latest Oligocene, Mackenzie Bay Sequence

Figure 16c. *Bathysiphon*, GSC 112288, Amauligak J-44, 2780 m Oligocene, Kugmallit Sequence

Figure 16d. *Bathysiphon*, GSC 112288 [see Fig. 16c]

Figure 16e. *Recurvoides*, GSC 112289, Amauligak J-44, 3599 m, Oligocene, Kugmallit Sequence

Figure 16f. *Labrospira*, GSC 112290, Amauligak J-44, 3599 m, Oligocene, Kugmallit Sequence

Figure 16g. *Haplophragmoides*, [GSC 112236, see Fig. 6c]

Figure 16h. *Marginulina*, [GSC 112238, see Fig. 7b]

Figure 18a. *Lenticulina*, GSC 112291, Roland Bay L-41, 1586 m, Late Jurassic, Kingak Formation

Figure 18b. *Lenticulina*, GSC 112292, Roland Bay L-41, 1586 m, Late Jurassic, Kingak Formation

Figure 19a. *Bathysiphon*, GSC 112293, Roland Bay L-41, 670 m, Turonian, Boundary Creek Formation

Figure 19b. *Marginulina*, GSC 112294, Roland Bay L-41, 2682 m, Late Jurassic, Kingak Formation

Figure 20. *Reticulophragmium*, GSC 112295, Amauligak J-44, 3998 m, Oligocene, Kugmallit Sequence